NASA CONTRACTOR REPORT

NASA CR-615

AN EXPLORATORY STUDY OF INTERNALLY AND EXTERNALLY FINNED RADIATORS FOR BRAYTON CYCLES IN SPACE

by S. V. Manson

Prepared by
S. V. MANSON & COMPANY, INC.
Arlington, Va.
for Lewis Research Center

NATIONAL AERONAUTICS AND SPACE ADMINISTRATION • WASHINGTON, D. C. • MARCH 1967

NASA CR-615

AN EXPLORATORY STUDY OF INTERNALLY AND EXTERNALLY FINNED RADIATORS FOR BRAYTON CYCLES IN SPACE

By S. V. Manson

Prepared under Contract No. NAS 3-2535 by
S. V. MANSON & COMPANY, INC.
Arlington, Va.

for Lewis Research Center

NATIONAL AERONAUTICS AND SPACE ADMINISTRATION

For sale by the Clearinghouse for Federal Scientific and Technical Information
Springfield, Virginia 22151 – CFSTI price $3.00

FOREWORD

The research described herein was conducted by S. V. Manson & Company, Inc., under NASA Contract No. NAS 3-2535. Mr. Martin Gutstein, Space Power Systems Division, NASA Lewis Research Center, was Technical Manager.

Table of Contents

AN EXPLORATORY STUDY OF INTERNALLY AND EXTERNALLY FINNED RADIATORS FOR BRAYTON CYCLES IN SPACE

S. V. Manson

SUMMARY

Sizes and weights are computed for Brayton cycle radiators that use a gas as their working fluid. The effects of fins on the inside surfaces of the radiator tubes are evaluated. The effects of annular fins on the outside surfaces of the radiator tubes are discussed.

The calculations indicate that internally finned radiators are more than 15 percent lighter in weight and more than 35 percent smaller in size than are internally unfinned radiators.

The calculations suggest that radiators equipped with annular external fins may be smaller in size than radiators equipped with central-type external fins.

INTRODUCTION

The Brayton cycle, which employs a gas as the turbomachinery working fluid, is one of the thermodynamic cycles being considered for the conversion of heat to electrical power in space applications (Ref. 1). Two major reasons for considering the Brayton cycle are (1) that there exists a large background of successful experience

with gas cycle turbomachinery and (2) that the use of a gas avoids fluid flow, heat transfer, component and materials problems that may require solution with two-phase fluids in space.

One possible arrangement of the Brayton cycle is shown schematically in figure 1. In this arrangement the working gas goes through the following processes:

(a) It is heated in the heat source;

(b) Flows to the turbine, where it expands and delivers to the turbine the energy required to drive the compressor and alternator;

(c) Flows to the recuperator, where it transfers heat to a relatively cool portion of the cycle gas stream;

(d) Flows to the radiator, where it discards the waste heat of the cycle;

(e) Flows to the compressor, where its pressure and temperature are raised;

(f) Flows to the recuperator, where it is heated;

(g) Flows to the heat source, where it is heated further (Step (a)).

The gas goes through Steps (a)-(g) repeatedly. For the present study, Step (d) is of primary interest; this Step indicates that the working fluid in the radiator is a gas.

When the working fluid in the waste heat radiator is a gas, the radiator size, weight and reliability are affected by the following properties of the gas: (1) Gases are relatively poor heat transfer fluids; (2) gases have low densities and require relatively large

flow areas in order to avoid high pressure drop and substantial pumping power; (3) gases experience a temperature drop during flow through the radiator with an associated decrease in the radiating potential of the armor and fins.

The cited gas properties could lead to large, heavy and thermally stressed waste heat radiators.

The aims of the present study are as follows:

(a) To develop a method of computing the dimensions and weights of radiators that use a gas as their working fluid;

(b) To employ this method to evaluate two concepts for reducing size, weight and stress in such radiators. The first concept involves the use of conducting fins on the gas-swept inner surfaces of the radiator tubes. The second concept involves the use of annular radiating fins on the external surfaces of the radiator tubes. The effects on radiator size and weight are evaluated quantitatively. The effects on thermal stress are discussed qualitatively.

The general radiator arrangement within which the foregoing concepts are evaluated is shown in figure 2. The radiator consists of an assembly of tubes lying in a single plane and radiating heat to space on both sides of the plane. Gas is fed to the tubes by a supply header and is removed from the tubes by an exhaust header; both headers are tapered. Within the tubes the gas transfers heat by

convection to the tube inner surfaces. The heat then flows by conduction across the tube walls, which are thick enough to serve as armor against penetration by meteoroids. Part of the heat is radiated to space by the outer surface of the armor; the rest of the heat is conducted to external fins attached to the outer surface of the armor and is radiated to space by these fins.

In the present study, the radiator tubes of figure 2 are assumed to be finned internally, as well as externally. The tube internal geometries evaluated are shown in cross section in figure 3. Figure 3 shows four internally finned tube geometries, and also the internally bare (unfinned) tube geometry that was computed for reference purposes. The external fin configurations evaluated are shown in figures 4 and 5. Figure 4 illustrates conventional central-type external fins; figure 5 illustrates circumferential (annular)-type external fins.

In relation to the configurations shown in figures 2 - 5, the aims of this study may be stated in detail as follows:

1. To develop a method of computing the sizes and weights of armored, externally finned, headered radiators that are arranged as in figure 2 and that operate non-isothermally with a gaseous working fluid.

2. For a prescribed set of operating conditions, and for tubes equipped with central external fins, to compute the sizes and weights

of both internally finned and internally unfinned radiators.

3. To compare the sizes and weights of the internally finned radiators with the sizes and weights of the internally unfinned radiators.

4. To consider briefly the potential gains from use of external radiating fins of annular shape.

In the calculation procedure developed, the radiator parts are computed in a definite sequence, as follows: (1) armor, (2) external fins, (3) headers, (4) radiator size and weight.

The armor details are computed with "mechanical" (i.e., non-thermal) equations. The external fins are computed by use of basic fin-and-tube data of the sort available in References 2 and 3. The headers are computed on the basis of gas velocity and pressure drop considerations. Heat transfer from the headers is neglected; the outside surface area of the headers is calculated, however, and is used as a basis for estimating the final thickness of the armor on the tubes and headers of the radiator.

The calculation procedure is applicable to armored-tube radiators with a wide variety of external fin geometries. For ease of calculation, the present study is limited to the special class of radiators for which the ratio of the heat dissipated by the external fins to the heat dissipated by the armor is the same at every axial station.

Radiators composed entirely of aluminum are assumed. Tube inside diameters ranging from about 0.3 to about 3.4 inches, and tube lengths of 6 and 25 feet, are evaluated. In each of the internally finned tubes the number of fins per tube is varied over a substantial range; the total range covered for the various internally finned geometries is 4 to 70 fins per tube. In all cases the assumed thickness of the internal fin metal is .004 inch. For the class of radiators considered, the thickness of the external fins decreases in the direction of the gas flow if the fin length (or diameter) and fin conductance parameter are both kept constant for the entire radiator. Constant fin length (or diameter) and constant fin conductance parameter are assumed in the present report; several values of the conductance parameter are considered for each of the two external fin types evaluated.

APPROACH

To calculate radiators of the type illustrated in figure 2, the approach used in this study is divide the radiator into several parts and to compute each part separately in a definite sequence. The sequence is chosen so as to permit the calculation of each part from existing or previously established information. Wherever possible, use is made of integral relations and end states to design each component in its entirety, rather than to pursue step-by-step calculation procedures.

The parts into which the radiator is divided are as follows: (a) the internal fins (if any); (b) the armored tubes through which the gas flows; (c) the external fins; (d) the headers. The parts are calculated in the order listed. Qualitative descriptions of the procedures employed are as follows:

The geometric arrangement and the detailed dimensions of the internal fins are treated as input.

The tubular armor is treated in part as input, and in part as output. The tube inside diameter and the tube length are assigned; the number of tubes and the armor thickness are computed. The equations employed to compute the number of tubes and the armor thickness are (1) the gas pressure drop equation, (2) the one-dimensional gas continuity equation, (3) the equation that defines the armor thickness for a prescribed degree of protection against penetration by meteoroids, and (4) a purely geometric equation that relates the armor surface to the number of armored tubes, their length, their inside diameter and wall thickness. The wall thickness computed in this way corresponds, from the viewpoint of meteoroid protection, to the exposed outer surface of the tubes alone; a correction to the wall thickness is added later, when the exposed surface of the headers has been computed.

With the armor geometry known except for a refinement of its thickness, the calculation proceeds to the external fins. Part of the information needed to fix the external fin dimensions is obtained by introducing the thermal equations of the armor. The armor thermal equations, together with independently available

external fin data, are employed to determine the dimensions of the external fins required for thermal compatibility with the already computed armor. In the present study the armor equations and the external fin data are formulated in terms of a heat ratio, namely, the ratio of the heat radiated jointly by the armor and the external fins, to the heat that would be radiated at the same temperature by the armor alone if the external fins were absent. This ratio, which in the general case would vary in magnitude from one point to another along the armor of a non-isothermal radiator, is denoted by the symbol $(dQ)/(dQ_b^*)$. (All symbols are defined in Appendix A.)

For simplicity, the calculations in this report are confined to the class of radiators for which the ratio $(dQ)/(dQ_b^*)$ is a constant for the entire radiator. The basic data of References 2 and 3, expressed in terms of $(dQ)/(dQ_b^*)$, are employed to determine the dimensions of central and circumferential types of external fins that are compatible with the armor geometries of this class of radiators. Graphical maps are used to facilitate the calculations. Axial temperature variation is taken into account.

With both the armor geometry and external fin dimensions known, the associated header lengths are readily computed. The headers are designed to provide the same bulk fluid velocity at all axial stations; hence, the headers are tapered along their length. The entrance and exit diameters are determined by the requirement that the fluid pressure drop shall be a prescribed value. The header surface areas are also computed and are used as a basis

for estimating the final value of the armor thickness on the radiator tubes and headers. Heat transfer from the header surfaces is not taken into account in the calculation procedure.

With all details known, the radiator total size and weight are computed straightforwardly. The sizes and weights of internally finned radiators are then compared with the sizes and weights of internally unfinned radiators. Similarly, the sizes and weights of radiators equipped with circumferential external fins are compared with the sizes and weights of radiators equipped with central external fins.

CALCULATION PROCEDURE

The equations of the calculation procedure are indicated in this section. In addition, the input and output quantities of the calculation and the major underlying assumptions are indicated.

Input Quantities

The input consists of the following items (symbols are defined in Appendix A):

Gas operating conditions: Gas composition and $\dot{m}$; and T_{en}, T_{ex}, p_{en}, p_{ex} during flow through each of the following physical components-- the supply header, the radiator tubes and the exhaust header; also, data on c_p, μ and k as functions of T.

Internal fins (see figure 3): Material, geometric array, b, δ_f, n; correlations for heat transfer coefficients and friction factors in flow through channels containing such fins (see figure 6); and a formula or curve that permits evaluation of the fin effectiveness as a function of the parameter(s) on which the fin effectiveness depends.

Armor: Material, ϵ, d_i, l. Also input is a meteoroid criterion that permits calculation of armor thickness for prescribed values of P(0) and τ; the quantities P(0) and τ are input values. In the present study the meteoroid criterion of Reference 4 is employed.

External fins: Material, ϵ, general arrangement. In addition, for central-type external fins the input includes the conductance parameter (N_{c,L_F}) and curves of L_F/R_a versus $(dQ)/(dQ_b^*)$ at various values of N_{c,L_F} (see figure 7). For circumferential external fins, the input includes $R_{o,F}/R_a$ and curves of $(dQ)/(dQ_b^*)$ versus N_{c,R_a} at various values of s_F/R_a (see figure 8).

Headers: Gas operating conditions, wall composition, and specification whether the headers are unsplit or split (see figure 2).

Environment: T_e

Output Quantities

The following items are end results of the calculation:

Armor: N, δ_a, D_a, weight.

Internal fins: weight.

External fins: For central-type fins -- L_F , $\Delta_{F,x}$, weight. For circumferential type fins -- $R_{i,F}(=R_a)$, $R_{o,F}$, s_F , $\Delta_{F,x}$, number of fins, weight.

Headers: L_H, $d_{H,en}$, $d_{H,x}$, $d_{H,ex}$, weight. These quantities are obtained for both the supply header and the exhaust header.

Total radiator: Weight, planform area (including the incremental area contributed by the headers).

Assumptions

The following assumptions are made in order to facilitate analysis and calculations. Brief discussion of some of the assumptions is presented.

Assumption 1. In computing the friction pressure drop of the gas in a radiator channel, an average gas density may be used for the entire channel. This average density is assumed to be computable by use of the perfect gas law in conjunction with an average pressure and an average temperature given by

$$p_{av} = \frac{p_{en} + p_{ex}}{2} \tag{1}$$

$$\left.\begin{aligned} T_{g,av} &= C_T\left[\frac{T_{g,en} + T_{g,ex}}{2}\right] \\ C_T &\lesssim 1 \end{aligned}\right\} \tag{2}$$

Equation (1) is a reasonable assumption when the overall gas pressure drop is a moderate fraction (≤ 0.1) of the gas inlet pressure and there are no abrupt pressure changes within the channel. In the present study, $\Delta p/p_{en} \sim 0.05$, the gas velocities are subsonic, and abrupt pressure changes are not expected.

For this study, equation (2) was simplified by taking $C_T = 1$. Check calculations showed that at the radiator operating conditions considered, the use of $C_T = 1$ over-estimates the radiator sizes and weights by about 3 to 5 percent.

The assumption that an average gas density may be used for the entire channel makes possible the use of an integral form of the pressure drop equation. Thereby the assumption uncouples the required number of radiator tubes from details of the thermal history of the gas. Assumption 1 therefore plays an important role in the calculation procedure of the present study.

Assumption 2. A single (average) value of the gas heat transfer coefficient may be used everywhere in the radiator channels. In computing the average heat transfer coefficient, the physical properties of the gas may be evaluated at an average gas film temperature given by

$$T_{film} = \frac{T_{g,av} + T_{w,av}}{2} \qquad (3)$$

It is assumed that a satisfactory estimate can be made of $T_{w,av}$ -- if necessary, on the basis of a detailed initial calculation. Preliminary calculations indicated that $T_{film} \simeq 0.97\ T_{g,av}$ in the internally finned radiators of this study. The same value of T_{film} was used for the internally unfinned radiators of this report.

The assumption that an average gas heat transfer coefficient may be used for the entire radiator frees the heat transfer coefficient from the detailed thermal history of the gas. It also implies that a constant value of overall coefficient of heat convection-and-conduction, U, may be employed for the entire radiator. The constancy of U permits the extraction of U from under an integral sign that arises in a thermal equation of the armor.

Assumption 3. At every tube cross section, the tube wall temperature is uniform around the circumference.

This assumption facilitates calculations; it permits the use of numerical data presented in References 2 and 3 for determining the dimensions of the external fins.

Assumption 4. Axial heat conduction is negligible.

Reference 5 has shown that axial conduction effects are negligible in the external (radiating) fins of practical radiators, and that axial temperature variation affects negligibly the radiant heat interchange between radiator elements. Reference 5 does not study the effects of axial conduction in the tube wall. A detailed study of such effects is outside the scope of the present analysis.

Assumption 5. The emissivity and absorptivity of the armor and of the external fins are uniform over the entire radiator.

Assumption 6. The effective environment temperature is the same for all parts of the radiator.

Assumption 7. The geometry in the interior of the gas channels is the same throughout the radiator.

Principal Equations

Internal Fins

The geometry and dimensions of the internal fins are input data. Relations involving the internal fins are presented in the first sub-section under "Armor".

Armor

Basic relations for the tube interior:

$$A_{\text{flow per tube}} = \frac{\pi}{4} d_i^{\,2} - (\text{Blocked area per tube}) \tag{4}$$

$$\begin{pmatrix}\text{Blocked area} \\ \text{per tube}\end{pmatrix} = \left(\begin{array}{l}\text{Sum of the cross sectional areas of all fin metal parts and of internal blockage tube (if any), computed at any tube cross section taken perpendicular to the tube axis; see figure 3.}\end{array}\right) \tag{5}$$

$$P_{w \text{ per tube}} = \left(\begin{array}{l}\text{Sum of the perimeters of those parts of the tube, fins and blockage tube (if any) that are contacted by the gas, computed at any tube cross section taken perpendicular to the tube axis; see figure 3.}\end{array}\right) \tag{6}$$

$$d_{eq} \equiv 4\left(\frac{A_{\text{flow per tube}}}{P_{w \text{ per tube}}}\right) \tag{7}$$

$$\frac{S_f}{S_{w,i}} \equiv \frac{\left(\begin{array}{l}\text{Sum of the wetted perimeters of all fins in}\\ \text{any one tube cross section, excluding the fin}\\ \text{bases and their exposed sides; see figure 9(a).}\end{array}\right)}{\left(\begin{array}{l}\text{Wetted perimeter of tube wall at the same}\\ \text{cross section, including the fin bases and}\\ \text{their exposed sides; see figure 9(a).}\end{array}\right)} \qquad (8)$$

The definition in equation (8) treats the fin base, which attaches the fin to the tube wall (see figure 9), as a portion of the tube wall. This is a close approximation if the fin thickness, δ_f, is very small in comparison with the tube radius, r_i, and in comparison with the fin dimension, b (see figure 9(b)). In the present study, the ratio δ_f/r_i is $\lesssim 0.01$, and the ratio δ_f/b is $\lesssim 0.03$. For geometries in which the fins are formed by extrusion and there is no fin base, the wetted perimeter of the fin base (and of its sides) is zero, and equation (8) also applies.

For internally unfinned tubes, all terms involving internal fins in the foregoing equations have the value zero.

The mass flow per unit flow area in the tube is

$$G = \frac{\dot{m}}{N\, A_{\text{flow per tube}}} \qquad (9)$$

The film Reynolds number of the flow is

$$Re_{film} = \frac{G\, d_{eq}}{\mu_{film}} \frac{T_{av}}{T_{film}} \qquad (10)$$

For assumed uniform gas flow distribution in the tubes, G and Re_{film} are the same for all the tubes.

The one-dimensional continuity equation for flow in tubes of constant cross sectional area is

$$G = (\rho v)_x = \text{constant} \tag{11}$$

The drop in static pressure experienced by the gas in flow through the tubes is given by

$$\Delta p = \left|\Delta p_{fr}\right| + \Delta p_{momentum} \tag{12}$$

From a generalization of the results of Reference 6 for flow through tubes,

$$\begin{aligned} \left|\Delta p_{fr}\right| &= 4 f_{film} \frac{l}{d_{eq}} \frac{\rho_{film} v_{av}^2}{2g} \\ &= 4 f_{film} \frac{l}{d_{eq}} \frac{(\rho_{av} T_{av}/T_{film}) v_{av}^2}{2g} \end{aligned} \tag{13}$$

In equation (13), the friction factor depends on the internal geometry of the tube and on Re_{film}, and for each internal geometry is obtained from a functional relation of the form

$$f_{film} = \text{function of } Re_{film} \quad \text{(see figure 6)} \tag{14}$$

Also, from the basic definition of pressure change accompanying changes in the momentum of a gas during flow through a channel of constant cross-sectional area,

$$\Delta p_{momentum} = \left[\left(\frac{\rho_{ex} v_{ex}}{g}\right)v_{ex} - \left(\frac{\rho_{en} v_{en}}{g}\right)v_{en}\right] \qquad (15)$$

The gas heat transfer coefficient depends on the internal geometry of the tube, on the Prandtl number of the fluid and on Re_{film}, and for each internal geometry is obtained from a functional relation of the form

$$\left(\frac{h}{c_{p,av}G}\right) Pr_{film}^{2/3} = \text{function of } Re_{film} \text{ (see figure 6)} \qquad (16)$$

The heat transfer coefficient determined by equation (16) applies to both the tube surface and fin surface in the tube interior.

For internal fins of the types considered in the present study, the fin effectiveness is given by the following equation (Ref. 7):

$$\eta_f = \frac{\tanh\left(b\sqrt{\frac{2h}{k_f \delta_f}}\right)}{\left(b\sqrt{\frac{2h}{k_f \delta_f}}\right)} \qquad (17)$$

The total effective heat transfer surface in the tube interiors is

$$S_{eff} = S_{w,i} + \eta_f S_f \tag{18}$$

The effective conductance of the gas is

$$\left.\begin{aligned} (hS)_{eff} &= h(S_{w,i} + \eta_f S_f) \\ &= \left[h\left(1 + \eta_f \frac{S_f}{S_{w,i}}\right)\right] S_{w,i} \end{aligned}\right\} \tag{19}$$

Equation (19) shows that the effective heat transfer coefficient relative to the inner surface of the tube walls, (i.e., relative to $S_{w,i}$), is

$$h_{eff} = h\left(1 + \eta_f \frac{S_f}{S_{w,i}}\right) \tag{20}$$

For internally unfinned tubes, $\eta_f = 0$ in equations (17)-(20).

The foregoing equations, together with the perfect gas law and equations (1)-(3) presented in the Assumptions, comprise the basic elements of calculation insofar as the interior of the gas channels is concerned.

The first steps of the calculation consist of using the input gas data to compute p_{av}, T_{av} and T_{film} with equations (1)-(3) of the Assumptions. The bulk average density, ρ_{av}, is then computed with the perfect gas law in conjunction with p_{av}, T_{av} and the gas constant corresponding to the gas composition stipulated in the input. The pertinent gas properties are then determined on the basis of T_{av} and T_{film} (equation (16)). Also computed are the inlet and exit gas densities, ρ_{en} and ρ_{ex}, for the supply header, the radiator tubes and the exhaust header.

The input geometric data for the internal fins and for the inside diameter of the armor are then employed in equations (4)-(8) to compute $A_{flow\ per\ tube}$, d_{eq}, and $S_f/S_{w,i}$.

With d_{eq}, μ_{film} and T_{av}/T_{film} known, equation (10) is written in the forms

$$Re_{film} = \text{const.} \times G, \quad \text{or,} \quad G = \text{const.} \times Re_{film}$$

which permit immediate determination of the value of G associated with any value of Re_{film}. Additionally, equations (14) and (16), used together with data of the sort presented in figure 6, permit determination of unique values of f_{film} and h associated with each Re_{film} in channels of prescribed internal geometry.

Calculation sequences based on the foregoing equations are detailed in the following paragraphs.

Number of tubes: The number of tubes is determined by joint use of the gas continuity and gas pressure drop equations, (11) and (12)-(15), in conjunction with input data, as follows:

When equation (11) is inserted into equations (13) and (15), equation (12) takes the familiar form

$$\Delta p = 4 f_{film} \frac{l}{d_{eq}} \frac{G^2}{2g \rho_{av}} \frac{T_{av}}{T_{film}} + \frac{G^2}{g \rho_{en}} \left(\frac{\rho_{en}}{\rho_{ex}} - 1 \right) \qquad (21)$$

In equation (21), the quantities Δp and l are input data, and the gas densities, T_{av}/T_{film} and d_{eq} are known from calculations based on input data. Thus in equation (21), only f_{film} and G are unknown. Now the discussion at the end of the foregoing section indicates that for known μ_{film}, T_{av}/T_{film} and d_{eq} in channels of prescribed internal geometry, both f_{film} and G are uniquely determined for each value of Re_{film}. Hence, equation (21) is solved for G (and for f_{film}) by iteration of Re_{film}. Thus G becomes known.

For known G, the number of tubes is computed with equation (9), re-written in the form

$$N = \left(\frac{\dot{m}}{A_{flow\ per\ tube}} \right) \frac{1}{G} \qquad (22)$$

in which $\dot{m}$ is known as input and $A_{flow\ per\ tube}$ is known from previous calculations (eq. (4)). In a final radiator design, N must be an integer.

Armor surface and thickness: The armor surface and the associated thickness are determined by joint use of an input meteoroid criterion and a purely geometric equation for the exposed surface of the tubes:

The armor thickness required to protect the exposed surface of the radiator tubes is (Ref. 4)

$$\delta_a = C_a S_a^{1/3\beta} \tag{23}$$

in which C_a and β are input constants; C_a is given by

$$C_a = 2a \left(\frac{\rho_p}{\rho_t}\right)^{1/2} \left(\frac{\bar{V}}{c}\right)^{\theta} \left(\frac{.00421}{\rho_p}\right)^{1/3} \left(\frac{\alpha\tau}{-\ln P(0)}\right)^{1/3\beta} \left(\frac{2}{3\theta\beta + 2}\right)^{1/3\beta} \tag{24}$$

In the present study the following input values were used:

$a = 1.75$

$\rho_p = 27.46$ lb/ft^3

$\bar{V} = 9.84 \times 10^4$ ft/sec

$\alpha = 5.3 \times 10^{-11}$ gm$^{\beta}$/(ft^2 day)

$\beta = 1.34$

$\theta = 2/3$

The speed of sound in the armor material, c, was computed with the following formula:

$$c = \sqrt{\frac{gE}{\rho_t}} \tag{25}$$

The armor material was assumed to be aluminum. The following values were inserted into equation (25) :

$g = 32.2 \ \frac{lb_m}{lb_f} \ \frac{ft}{sec^2}$

$E = 144 \times (10.5 \times 10^6) \ lb_f/ft^2$ at an average armor surface temperature of approximately 675 ^oR (Ref. 8, Figure 10)

$\rho_t = 172 \ lb_m/ft^3$ (Ref. 8, Table I)

The value of c computed with equation (25) was as follows:

$c = 1.68 \times 10^4$ ft/sec

The values employed for P(0) and τ were as follows:

$P(0) = 0.9$

$\tau = 365$ days

With these input values equation (23) becomes

$$\delta_a(ft) = 0.00413 \ S_a^{0.249} \tag{26}$$

The purely geometric formula for the tube outer surface, S_a , is

$$S_a = N\left[\pi(d_i + 2\delta_a)l\right] \tag{27}$$

In equation (27), the quantities d_i and l are known as input, and N is known from equation (22); the armor surface S_a and thickness δ_a are unknown.

Equations (23) and (27) are two simultaneous equations in the two unknown S_a and δ_a. The joint solution of these two equations yields S_a and δ_a. The armor thickness computed in this way corresponds to the exposed surface of the tubes alone; a correction to δ_a is added later, after the exposed surface of the headers has been computed.

Since the internal fin dimensions and d_i and l are known as input, the solutions for N and δ_a complete the design of the armored radiator tubes (except for the refinement in δ_a required to allow for the exposed surface of the headers).

In the foregoing armor design procedure, no reference has been made to specific details of gas temperature or gas pressure within the radiator channels. Microscopic examination of in-tube gas states has been unnecessary because detailed fluid thermal and pressure histories enter into consideration only to the extent that they affect the value of the term $\rho_{av}/(T_{av}/T_{film})$ in equation (21). In the present study it has been assumed that $\rho_{av}/(T_{av}/T_{film})$ can be computed conservatively by use of equations (1) - (3).

The disregard of detailed gas states within the tubes does not imply that information on the local gas states cannot be obtained by the present calculation procedure. Such information is obtainable and can be used to check the assumption that $\rho_{av}/(T_{av}/T_{film})$ is conservatively estimated by use of equations (1) - (3). The information can also be used to compute more exact values of p_{av} , T_{av} and T_{film} , when more exact calculations are required. Detailed values of in-tube gas temperatures, which can also be used to compute the in-tube pressure field, become available as a by-product of the determination of armor surface temperatures. The armor surface temperatures are needed for design of the external fins. Thermal relations for the armor are presented in the following section.

Armor thermal relations: The following formulas are used for determining the axial temperature distributions of the outer surface of the armor and of the gas within the tubes; and also for determining the value of the parameter $(dQ)/(dQ_b^*)$ which, together with the armor surface temperatures, controls the design of the external fins. The formulas are based on heat balances and are derived in Appendix B.

For tube internal geometries of the sort shown in figure 3, the overall coefficient of heat convection-and-conduction from the gas

within the tubes to the outer surface of the armor is given by

$$U = \frac{h_{eff}\left(1 - \frac{\delta_f}{d_i}\right)}{\left(\frac{D_a}{d_i}\right) + h_{eff}\left(1 - \frac{\delta_f}{d_i}\right)\frac{D_a}{2k_a}\ln\left(\frac{D_a}{d_i}\right)} \tag{28}$$

where

$$D_a = d_i + 2\delta_a \tag{29}$$

All terms in the right members of equations (28) and (29) are computable from previously calculated quantities, as follows:

The effective heat transfer coefficient of the gas, h_{eff}, is given by equation (20). In equation (20), the basic coefficient h is determined by use of equation (16), in which both G and Re_{film} are known from previous solution of equation (21); see also equation (10) and figure 6. Since h is known, the effectiveness of the internal fins, η_f, is computable with equation (17). Also, the ratio $S_f/S_{w,i}$ is known by use of equation (8) in conjunction with the input geometric data for the internal fins. Hence, all quantities required for determining h_{eff} are known.

The term δ_f/d_i is known from input data; and D_a is known from the previous solution for δ_a.

Thus U can be computed with equation (28).

The relation between the armor and gas temperatures at an axial station located a distance x from the inlet of the radiator tubes is now considered. For this purpose the term $(dQ)/(dQ_b^*)$ is introduced.

The term $(dQ)/(dQ_b^*)$ is a ratio of two infinitesimal heat releases. The quantity dQ is the total heat radiated by a differential element of armor-plus-external fins when the outer surface temperature of the armor is $T_{a,x}$. The quantity dQ_b^* is the heat that would be radiated by the same armor surface element if the external fins were removed but the armor were maintained at the temperature $T_{a,x}$.

When the armor thermal equations are expressed in terms of the ratio $(dQ)/(dQ_b^*)$, the same basic forms of the equations may be used with a wide variety of external fin geometries.

For ease of calculation, the present study is limited to the class of radiators for which $(dQ)/(dQ_b^*)$ is a constant for the entire radiator. The following formulas are therefore specialized forms of the more general ones that apply when $(dQ)/(dQ_b^*)$ varies from point to point along the radiator. The following equations apply only to the class of radiators for which $(dQ)/(dQ_b^*)$ has the same value at every station of the armor surface.

The armor outer surface temperature at a distance x from the inlet station of the radiator tube is given by the equation

$$T_{a,x} + \sigma\epsilon\left[\frac{(dQ)/(dQ_b^*)}{U}\right]T_{a,x}^4 = T_{g,x} + \sigma\epsilon\left[\frac{(dQ)/(dQ_b^*)}{U}\right]T_e^4 \qquad (30)$$

In equation (30) the quantities σ, ϵ, T_e and U have known values. The quantity $(dQ)/(dQ_b^*)$, although constant for the entire radiator, is unknown and has to be determined by calculation, as detailed below. The gas temperature, $T_{g,x}$, has the following properties:

(a) $T_{g,x}$ may be assigned any value in the temperature interval $T_{g,en} \geq T_{g,x} \geq T_{g,ex}$, but the station x at which the assigned value of T_g occurs is not generally known beforehand and has to be found by calculation; a method of solving for x is detailed below. The fact that x is initially unknown does not prevent solution of equation (30) for $T_{a,x}$, because x does not appear in explicit form in the equation.

(b) There are two values of T_g for which x is known initially, namely,

$$\left.\begin{aligned} T_g &= T_{g,en} \quad \text{at} \quad x = 0 \\ T_g &= T_{g,ex} \quad \text{at} \quad x = l \end{aligned}\right\} \tag{31}$$

At $x = 0$ and l, that is, at the radiator tube entrance and exit station respectively, equation (30) takes the forms

$$T_{a,en} + \sigma\epsilon\left[\frac{(dQ)/(dQ_b^*)}{U}\right]T_{a,en}^4 = T_{g,en} + \sigma\epsilon\left[\frac{(dQ)/(dQ_b^*)}{U}\right]T_e^4 \tag{32}$$

$$T_{a,ex} + \sigma\epsilon\left[\frac{(dQ)/(dQ_b^*)}{U}\right]T_{a,ex}^4 = T_{g,ex} + \sigma\epsilon\left[\frac{(dQ)/(dQ_b^*)}{U}\right]T_e^4 \tag{33}$$

In equations (32) and (33), the value of $(dQ)/(dQ_b^*)$ is unknown. An auxiliary relation is required for determining $(dQ)/(dQ_b^*)$. Such a relation is supplied by the thermal equation for the armor surface area.

For radiators in which $(dQ)/(dQ_b^*)$ is constant, the surface exposed by the armor to space in the axial distance from the radiator tube inlet to the station at x is given by

$$S_{a,x} = \frac{\dot{m}c_p}{(dQ)/(dQ_b^*)} \frac{1}{\sigma\epsilon} \frac{1}{4T_e^3} \left\{ \left[\ln \left(\frac{T_{a,x} + T_e}{T_{a,en} + T_e} \frac{T_{a,en} - T_e}{T_{a,x} - T_e} \right) + 2\tan^{-1}\left(\frac{T_{a,x}}{T_e}\right) - 2\tan^{-1}\left(\frac{T_{a,en}}{T_e}\right) \right] + \frac{\dot{m}c_p / \left[(dQ)/(dQ_b^*)\right]}{U / \left[(dQ)/(dQ_b^*)\right]} \ln \left(\frac{T_{a,en}^4 - T_e^4}{T_{a,x}^4 - T_e^4} \right) \right\} \quad (34)$$

The total surface of the armor, S_a, is obtained by substituting $T_{a,ex}$ for $T_{a,x}$ wherever $T_{a,x}$ appears in equation (34). On performing the substitution of $T_{a,ex}$ for $T_{a,x}$ in (34), and on then re-arranging the resulting expression, the following equation is obtained for $(dQ)/(dQ_b^*)$:

$$\frac{(dQ)}{(dQ_b^*)} = \frac{1}{U/\left[(dQ)/(dQ_b^*)\right]} \frac{\dot{m}c_p}{S_a} \ln\left(\frac{T_{a,en}^4 - T_e^4}{T_{a,ex}^4 - T_e^4}\right)$$

$$+ \frac{\dot{m}c_p}{S_a} \frac{1}{\sigma \epsilon} \frac{1}{4T_e^3} \left[\ln\left(\frac{T_{a,ex} + T_e}{T_{a,en} + T_e} \frac{T_{a,en} - T_e}{T_{a,ex} - T_e}\right) + \right\} \quad (35$$

$$+ 2\tan^{-1}\left(\frac{T_{a,ex}}{T_e}\right) - 2\tan^{-1}\left(\frac{T_{a,en}}{T_e}\right)\Bigg]$$

Equations (32), (33) and (35) are three simultaneous equations involving the unknown, $(dQ)/(dQ_b^*)$. It is recalled that in these equations, $\dot{m}c_p$ is an input quantity and the numerical values of U and S_a are known from previous calculations. The solution for $(dQ)/(dQ_b^*)$ is obtained from equations (32), (33) and (35) by iterating with trial values of $(dQ)/(dQ_b^*)$, as follows:

A trial value of $(dQ)/(dQ_b^*)$ is assigned and the corresponding value of $U/\left[(dQ)/(dQ_b^*)\right]$ is computed. The value of $U/\left[(dQ)/(dQ_b^*)\right]$ is inserted into equations (32) and (33) and these equations are solved for $T_{a,en}$ and $T_{a,ex}$. The values of $U/\left[(dQ)/(dQ_b^*)\right]$, $T_{a,en}$ and $T_{a,ex}$ are then inserted into the right side of equation (35), and the trial value of $(dQ)/(dQ_b^*)$ is inserted into the left side of

equation (35). The numerical values of the left and right sides of equation (35) are then compared. The value of $(dQ)/(dQ_b^*)$ that makes the left and right sides of equation (35) numerically equal to each other, within the desired degree of accuracy, is the solution for $(dQ)/(dQ_b^*)$.

When the solution for $(dQ)/(dQ_b^*)$ has been determined, the associated value of $U/[(dQ)/(dQ_b^*)]$ is inserted into equation (30). A series of values is assigned to $T_{g,x}$ in the range $T_{g,en} \geq T_{g,x} \geq T_{g,ex}$, and for each assigned value of $T_{g,x}$ the associated value of $T_{a,x}$ is computed with equation (30). In this way a series of paired values $(T_{g,x}, T_{a,x})$ is obtained.

The location, x, at which each combination $(T_{g,x}, T_{a,x})$ occurs is obtained by inserting the value of $T_{a,x}$ into equation (34), computing $S_{a,x}$, and solving for x with the relation

$$\frac{x}{l} = \frac{S_{a,x}}{S_a} \tag{36}$$

The foregoing procedure yields a unique solution for $(dQ)/(dQ_b^*)$, and numerical values of armor and gas temperatures at known positions along the tube length.

With the axial distribution of gas and armor temperatures known, it is possible (by joint use of these temperature distributions, the perfect gas law and the pressure drop equation in differential form), to check and refine equations (1), (2) and (3), and thereby to produce more exact solutions for N, S_a, δ_a, $(dQ)/(dQ_b^*)$, $T_{g,x}$, and $T_{a,x}$. When the pressure drop of the gas is small, it is adequate

to refine only T_{av} and T_{film} , equations (2) and (3).

The radiator sizes and weights presented in this report correspond to the initially assumed value of $\rho_{av}/(T_{av}/T_{film})$, computed on the basis of equations (1) - (3). Check calculations showed that the radiators of this report are about 3 to 5 percent larger and heavier than would be computed on the basis of a more exact value of $\rho_{av}/(T_{av}/T_{film})$.

External Fins

With $(dQ)/(dQ_b^*)$ and armor temperatures determined as in the foregoing section, the calculation of the external fins is performed by joint use of $(dQ)/(dQ_b^*)$, $T_{a,x}$, and independently available data that relate the fin dimensions to their thermal performance as measured by $(dQ)/(dQ_b^*)$. The calculation procedures employed for central and circumferential types of external fins are indicated in the following sub-sections:

a) Central fins: A map of L_F/R_a versus $(dQ)/(dQ_b^*)$, with N_c, L_F as parameter, is shown for central fins in figure 7. The lines in figure 7 are based on the numerical values reported in Reference 2. For converting the values of Reference 2 to the form shown in figure 7, the following formula was applied to the data presented in figures 2, 3 and 4 of Reference 2:

$$\frac{(dQ)}{(dQ_b^*)} = \left(\begin{matrix}\text{Ordinate in fig. 4}\\ \text{of Ref. 2}\end{matrix}\right) + \frac{2}{\pi}\,\frac{1}{R_a/L_F}\left(\begin{matrix}\text{Ordinate in fig. 2}\\ \text{of Ref. 2}\end{matrix}\right)\left(\begin{matrix}\text{Ordinate in fig. 3}\\ \text{of Ref. 2}\end{matrix}\right)$$

This formula was obtained by dividing both sides of equation (24b) of Reference 2 by the quantity $\pi R_a/2L_F$. Figure 7 shows that L_F/R_a varies linearly with $(dQ)/(dQ_b^*)$ when N_{c,L_F} is held constant.

The values in figure 7, taken as they are from Reference 2, automatically include the effects of temperature drop along the transverse dimension of the fin, and the effects of radiation interchange between fin and tube surfaces.

To determine the fin length L_F , the abscissa scale of figure 7 is entered at the known value of $(dQ)/(dQ_b^*)$, and for any chosen N_{c,L_F} the value of L_F/R_a is read from the ordinate scale. The fin length is given by

$$L_F = \left(\frac{L_F}{R_a}\right)R_a = \left(\frac{L_F}{R_a}\right)\frac{D_a}{2} \qquad (37)$$

In the present study, N_{c,L_F} and L_F were kept constant for each radiator. The quantity N_{c,L_F} was varied parametrically.

For known L_F, the thickness of the external fin at station x is computed from the definition of N_{c,L_F},

$$N_{c,L_F} = \frac{2\sigma T_{a,x}^3 L_F^2}{k_F \Delta_{F,x}} \tag{38}$$

which yields

$$\Delta_{F,x} = \frac{2\sigma T_{a,x}^3 L_F^2}{k_F N_{c,L_F}} \tag{39}$$

Equation (39) shows that when L_F and N_{c,L_F} are both kept constant, the fin thickness changes with the armor surface temperature. Since $T_{a,x}$ decreases axially, the fin thickness decreases from entrance to exit of the radiator. This is true only for radiators like those of the present study, in which $(dQ)/(dQ_b^*)$, L_F , and N_{c,L_F} all have values that remain the same from one axial station to the next along the armor surface.

The transverse span of a single centrally finned tube is $(D_a + 2L_F)$. For N tubes in parallel, the total span is $N(D_a + 2L_F)$, which is the header length for centrally finned radiators.

b) Circumferential external fins: A typical map that relates the spacing of circumferential external fins to $(dQ)/(dQ_b^*)$ and to N_{c,R_a} at a fixed value of R_o/R_a is presented in figure 8. The data in figure 8 are based on the results reported in Reference 3 and are

basically identical with the data of that Reference. In slight variations from the form employed by Reference 3 to present the data, different nomenclature is used herein, and figure 8 employs the ratio of fin spacing to fin inner radius as the curve identification parameter, instead of the ratio of fin spacing to fin outer radius employed by Reference 3. As the fin inner radius equals $D_a/2$ and is known explicitly from previous calculations, the inner radius is convenient for the present calculations and for this reason is used in the denominator of the curve identification parameter in figure 8.

The fin outer radius, fin axial spacing, fin thickness and number of fins per tube are determined as follows:

The ordinate scale in figure 8 is entered at the known value of $(dQ)/(dQ_b^*)$, and a line is drawn parallel to the axis of abscissas. This line intersects one or more curves of the figure, and each intersection point determines a combination of numerical values, s_F/R_a and N_{c,R_a} . It is evident that when $(dQ)/(dQ_b^*)$ is held constant, the consideration of more than one value of s_F/R_a is equivalent to parametric variation of N_{c,R_a}. With s_F/R_a and N_{c,R_a} both known, the fin dimensions and spacing are computed with the following formulas:

The fin outer radius is given by

$$R_o = \left(\frac{R_o}{R_a}\right)R_a = \left(\frac{R_o}{R_a}\right)\frac{D_a}{2} \qquad (40)$$

The fin axial spacing is given by

$$s_F = \left(\frac{s_F}{R_a}\right) R_a \tag{41}$$

The definition of the conductance parameter N_{c,R_a} for circumferential external fins is

$$N_{c,R_a} = \frac{2\sigma T_{a,x}^3 R_a^2}{k_F \Delta_{F,x}} \tag{42}$$

As indicated above, the numerical value of N_{c,R_a} is known for each combination of R_o/R_a , $(dQ)/(dQ_b^*)$ and s_F/R_a .

The fin thickness at station x is computed by the formula

$$\Delta_{F,x} = \frac{2\sigma T_{a,x}^3 R_a^2}{k_F N_{c,R_a}} \tag{43}$$

In the present study, N_{c,R_a} is kept axially constant in each radiator. Since $T_{a,x}$ decreases along the armor surface, the fin thickness $\Delta_{F,x}$ decreases steadily from entrance to exit stations along a radiator tube. This is true only for radiators like those of the present study, in which $(dQ)/(dQ_b^*)$, R_o/R_a , s_F/R_a and N_{c,R_a} are constants for the entire radiator.

The number of fins per tube is given by the adequate approximation

$$\nu = \frac{l}{s_F + \Delta_{F,av}} \tag{44}$$

in which $\Delta_{F,av}$ is the arithmetic average of the fin thicknesses at the entrance and exit stations of the radiator tube.

Note is taken that the foregoing formulas have been illustrated with curves for a single value of R_o/R_a (figure 8). In an exhaustive optimization study of circumferential external fins, exploration of several values of R_o/R_a is required, in search for the optimum value of R_o/R_a.

The transverse span of a single finned tube is $2R_o$. If N tubes are arranged in parallel in one plane so that the fins of adjacent tubes just touch each other, the combined transverse span of all the tubes is $N(2R_o)$, and this is the minimum possible header length of a circumferentially finned radiator in which the external fins do not mesh with or overlap each other.

Headers

In this study, the headers are designed for axially uniform drain-off from the supply header and axially uniform feed into the exhaust header. With the origin of x taken at the entrance plane of the supply header or, equivalently, at the exit plane of the exhaust header (figure 2), the conditions for uniform drain and uniform feed are expressed by the equation

$$\frac{d\dot{m}}{dx} = -\frac{\dot{m}_{H,en}}{L_H} = -\frac{\dot{m}_{H,ex}}{L_H} = \text{const.} \tag{45}$$

In addition, the condition is imposed that in each header the mass flow per unit cross-sectional area shall have the same value at every axial station of that header. This condition is expressed by the equations

$$\left.\begin{aligned} G_x = \left(\frac{\dot{m}}{A}\right)_x = \frac{\dot{m}_{H,en}}{A_{en}} = G_{en} = \text{const.} \\ \dot{m}_x = G_{en}\, A_x \end{aligned}\right\} \quad \left(\begin{matrix}\text{Supply} \\ \text{header}\end{matrix}\right) \tag{46a}$$

$$G_x = \left(\frac{\dot{m}}{A}\right)_x = \frac{\dot{m}_{H,ex}}{A_{ex}} = G_{ex} = \text{const.}$$

$$\dot{m}_x = G_{ex} A_x$$

$$\left.\begin{array}{l} \\ \\ \end{array}\right\} \left(\begin{array}{c}\text{Exhaust}\\ \text{header}\end{array}\right) \quad (46b)$$

Solution of equations (45) and (46) yields

$$d_{H,x} = d_{H,en} \sqrt{1 - \frac{x}{L_H}} \qquad \left(\begin{array}{c}\text{Supply}\\ \text{header}\end{array}\right) \qquad (47a)$$

$$d_{H,x} = d_{H,ex} \sqrt{1 - \frac{x}{L_H}} \qquad \left(\begin{array}{c}\text{Exhaust}\\ \text{header}\end{array}\right) \qquad (47b)$$

In equations (45) and (47) the header length L_H is known, as was indicated at the ends of the sub-sections on central and circumferential external fins; formulas for L_H are itemized explicitly soon hereafter. The diameters $d_{H,en}$ and $d_{H,ex}$ are initially unknown; they are computed by solution of the pressure drop equations for the gas in the supply and exhaust headers. Heat transfer in the headers is ignored in the present study, and the effect of heat transfer on the header diameters is not considered.

The gas flow in each header is treated separately and as though the flow were incompressible; different gas densities, based on the respective gas temperature-and-pressure combinations, are employed for the two headers. In each header the gas filament

that flows the full length of the header is assumed to experience a pressure drop based on three factors: (1) friction, (2) a loss of one dynamic head based on the velocity in the header, and (3) a loss of one dynamic head based on the velocity in the radiator tube and postulated to occur during passage from the supply header into the radiator tube or from the tube into the exhaust header. Gas filaments that flow only a portion of the length of the header are assumed to have the same pressure drop as the filament that flows the full length of the header; the smaller friction pressure drop in the flow along only a portion of the header length is assumed to be supplemented by pressure drop in calibrated orifices at the entrances and/or exits of the tubes. The friction component in the length interval (x, dx) is computed herein with the formulas for turbulent flow:

$$\left.\begin{aligned} dp_{fr} &= -4 f \frac{dx}{d_{H,x}} \frac{G_x^2}{2g\rho} \\ f &= \frac{0.046}{(G_x\, d_{H,x}/\mu)^{0.2}} \end{aligned}\right\} \qquad (48)$$

For each header ρ is treated as a constant; ρ is taken equal to ρ_{en} in the supply header, and is taken equal to ρ_{ex} in the exhaust header.

In order to compute the friction pressure drop of the gas filament that flows the full length of the header, equation (48) is integrated from x = 0 to L_H, making use of equations (46) and (47). The complete

pressure drop of the gas filament is then obtained by summing the friction term and the pertinent dynamic head losses, which are given by the following expressions:

The dynamic heads in the respective headers are given by

$$\frac{G^2}{2g\ \rho_{en}} = \frac{\dot{m}_{H,en}^2}{2g\ \rho_{en}\ (\pi/4)^2}\ \frac{1}{d_{H,en}^4} \qquad \left(\begin{matrix}\text{Supply}\\ \text{header}\end{matrix}\right) \tag{49a}$$

$$\frac{G^2}{2g\ \rho_{ex}} = \frac{\dot{m}_{H,ex}^2}{2g\ \rho_{ex}(\pi/4)^2}\ \frac{1}{d_{H,ex}^4} \qquad \left(\begin{matrix}\text{Exhaust}\\ \text{header}\end{matrix}\right) \tag{49b}$$

The dynamic heads based on the velocities in the radiator tube at the entrance and exit stations of the tube are given by

$$\text{Tube entrance dynamic head} = \frac{G_{tube}^2}{2g\ \rho_{en}} \tag{50a}$$

$$\text{Tube exit dynamic head} = \frac{G_{tube}^2}{2g\ \rho_{ex}} \tag{50b}$$

By setting the sum of the friction pressure drop and dynamic head losses in each header equal to the allowable pressure drop in the header, the following equations are obtained:

For the supply header,

$$\left.\begin{aligned} 2.5\left[\frac{4(.046)\mu_{en}^{0.2}\,\dot{m}_{H,en}^{1.8}}{2g\,\rho_{en}(\pi/4)^{1.8}}\right]\frac{L_H}{d_{H,en}^{4.8}} \;+\; \\ +\;\left[\frac{\dot{m}_{H,en}^{2}}{2g\,\rho_{en}(\pi/4)^{2}}\right]\frac{1}{d_{H,en}^{4}} \;+\; \frac{G_{tube}^{2}}{2g\,\rho_{en}} \\ =\quad \text{(Allowable supply header } \Delta p) \end{aligned}\right\} \qquad (51a)$$

and for the exhaust header,

$$\left.\begin{aligned} 2.5\left[\frac{4(.046)\mu_{ex}^{0.2}\,\dot{m}_{H,ex}^{1.8}}{2g\,\rho_{ex}(\pi/4)^{1.8}}\right]\frac{L_H}{d_{H,ex}^{4.8}} \;+\; \\ +\;\left[\frac{m_{H,ex}^{2}}{2g\,\rho_{ex}(\pi/4)^{2}}\right]\frac{1}{d_{H,ex}^{4}} \;+\; \frac{G_{tube}^{2}}{2g\,\rho_{ex}} \\ =\quad \text{(Allowable exhaust header } \Delta p) \end{aligned}\right\} \qquad (51b)$$

Equations (51a) and (51b) permit solution for $d_{H,en}$ and $d_{H,ex}$, respectively. In these equations, the allowable pressure drops for the supply and exhaust headers, the gas densities ρ_{en} and ρ_{ex}, and the viscosities μ_{en} and μ_{ex} in those headers, are known as input. The quantity G_{tube} is known from previous solution of

equation (21). The quantities $\dot{m}_{H,en}$ and $\dot{m}_{H,ex}$ are the total gas flow rates per branch in the entrance and exit headers. For unsplit headers as in figure 2a,

$$\left.\begin{aligned} \dot{m}_{H,en} &= \dot{m}_{H,ex} \\ &= \dot{m} \text{ of entire radiator} \end{aligned}\right\} \quad \left(\begin{matrix}\text{Unsplit} \\ \text{headers}\end{matrix}\right) \qquad (52a)$$

For split headers as in figure 2b,

$$\left.\begin{aligned} \dot{m}_{H,en} &= \dot{m}_{H,ex} \\ &= \frac{1}{2}(\dot{m} \text{ of entire radiator}) \end{aligned}\right\} \left(\begin{matrix}\text{Once-} \\ \text{split} \\ \text{headers}\end{matrix}\right) \qquad (52b)$$

If the headers were split into 2n branches, the flow rates per branch would be given by the relation

$$\dot{m}_{H,en} = \dot{m}_{H,ex} = \frac{1}{2n}(\dot{m} \text{ of entire radiator})$$

In equations (51a) and (51b), the header length L_H is as follows:

For central-type external fins (figure 4),

$$L_H = N(D_a + 2L_F) \qquad \text{(Unsplit headers)} \qquad (53a)$$

$$L_H = \frac{N}{2}(D_a + 2L_F) \qquad \text{(Once-split headers)} \qquad (53b)$$

For circumferential-type external fins (figure 5), the header length depends on the tube spacing required to avoid excessive mutual occlusion of the finned tubes when arranged in parallel. The minimum possible tube spacing for non-meshing fins is such that the fins of adjacent tubes just touch each other. Thus, for circumferentially finned tubes,

$$L_H \geq N(2R_o) \qquad \text{(Unsplit headers)} \qquad (54a)$$

$$L_H \geq \frac{N}{2}(2R_o) \qquad \text{(Once-split headers)} \qquad (54b)$$

In the present report the header lengths for circumferentially finned tubes were taken at the values corresponding to tangency of the fins of adjacent tubes; that is, the "equal" signs were used in equation (54). The extent to which the thermal performance of an array of N closely spaced tubes differs from the summed thermal performances of N isolated tubes requires detailed analysis outside the scope of the present report.

It may be noted that for headers split into 2n branches, the denominators in the right members of equations (53b) and (54b) would be 2n instead of the value 2 now shown.

With $d_{H,en}$ and $d_{H,ex}$ known by solution of equations (51a) and (51b), the total surface exposed by both headers combined is computed with the following formula, obtained by integrating

elements of surface $\pi(d_{H,x} + 2\delta_a)dx$ as x goes from 0 to L_H,

$$S_H = \pi L_{H,unsplit} \left[\left(\frac{2}{3} d_{H,en} + 2\delta_a\right) + \left(\frac{2}{3} d_{H,ex} + 2\delta_a\right)\right] \quad (55)$$

in which $L_{H,unsplit}$ is given by equation (53a) or (54a). Equation (55) applies both to unsplit headers and to headers split into any even number of identical branches, since the product $2n(L_{H,unsplit}/2n)$, which arises during consideration of split headers, always reduces to $L_{H,unsplit}$. The effect of splitting the headers is reflected in the diameters $d_{H,en}$ and $d_{H,ex}$, which become smaller as the number of header branches increases.

In equation (55) the armor thickness δ_a is taken equal to the value earlier obtained from joint solution of equations (23) and (27). A refinement of δ_a is considered in the following section.

Weights and Planform Area

The radiator total weight is the sum of the component weights, which are determined as follows:

The total surface exposed by the armored tubes and headers is given by the sum of the individual surfaces,

$$S_{a,total} = S_a + S_H \quad (56)$$

in which S_a is given by equation (27) and S_H by equation (55). Equations (27) and (55) are both initially based on the unrefined armor thickness δ_a obtained by joint solution of equations (23) and (27). A refined value of δ_a is obtained by inserting $S_{a,total}$ into equation (23):

$$\delta_{a,total} = C_a(S_{a,total})^{1/3\beta} \tag{57}$$

with C_a given by equation (24).

A more highly refined value of the armor thickness is obtainable by inserting the $\delta_{a,total}$ of equation (57) into the formulas for S_a and S_H, thereby refining $S_{a,total}$ and, through (57), $\delta_{a,total}$. With a more accurate value of $\delta_{a,total}$ thus available, the tube and header weights are as follows:

$$\begin{pmatrix}\text{Armored tube}\\ \text{wall weight}\end{pmatrix} = \rho_a\left[N l \pi (d_i + \delta_{a,total})\delta_{a,total}\right] \tag{58}$$

$$\left.\begin{pmatrix}\text{Total header}\\ \text{weight}\end{pmatrix} = \rho_a\left[\pi\delta_{a,total}\ L_{H,unsplit}\right] \times \times \left[\left(\frac{2}{3}D_{H,en} + \delta_{a,total}\right) + \left(\frac{2}{3}D_{H,ex} + \delta_{a,total}\right)\right]\right\} \tag{59}$$

In equation (59), the bracketed volume term is obtained by integrating volume elements of the form $\pi(d_{H,x} + \delta_{a,total})\delta_{a,total}dx$ as x goes

from 0 to L_H in each header. Equation (59) applies both to unsplit and split headers, for the same reason as was given in connection with equation (55).

The weight of the internal fins is given by

$$\begin{pmatrix}\text{Internal}\\ \text{fin weight}\end{pmatrix} = \left(\rho_f N l\right)\left[\begin{array}{l}\text{Sum of the cross-sectional}\\ \text{areas of all fin metal parts,}\\ \text{including fin bases, com-}\\ \text{puted at any single tube cross}\\ \text{section taken perpendicular}\\ \text{to the axis of the tube.}\end{array}\right] \qquad (60)$$

If the internal fins are brazed to the tube walls, the weight computed with equation (60) may be multiplied by 1.1 in order to make approximate allowance for the weight of the braze metal. If a flow blockage tube is present in the interior of the radiator tube (figure 3c), the weight of the blockage tube must also be included. In this study, no allowance was made for braze metal weight, but when a flow blockage tube was assumed to be present the weight of that tube was taken into account. The thickness of the blockage tube wall was taken as .005 inch and its material was assumed to be aluminum of density 172 lb/ft^3.

The weight of the external fins is affected by the fact that in the class of radiators studied, the thickness of the external fins decreases axially from entrance to exit of the radiator. Thus in computing the weight a properly averaged fin thickness must be

employed. When an average fin thickness is used, the weight of central-type external fins is given by

$$\begin{pmatrix}\text{External fin}\\ \text{weight}\end{pmatrix} = \rho_F \left[N l (2 L_F \Delta_{F,av}) \right] \qquad \begin{pmatrix}\text{Central}\\ \text{fins}\end{pmatrix} \tag{61}$$

The average thickness of axially tapered central-type external fins is given by the formula

$$\Delta_{F,av} = \frac{1}{l} \int_0^l \Delta_{F,x} dx \qquad \begin{pmatrix}\text{Central}\\ \text{fins}\end{pmatrix} \tag{62}$$

in which $\Delta_{F,x}$ is given by equation (39). For the present study, it was convenient to use an approximate value of $\Delta_{F,av}$, rather than the one defined by equation (62). The following approximate formula was employed:

$$\Delta_{F,av} \simeq \frac{(\Delta_F)_{\text{at } x=0} + 1.75\,(\Delta_F)_{\text{at } x=l}}{2.75} \tag{63}$$

Check calculations were made for the purpose of comparing the values of $\Delta_{F,av}$ given by equations (62) and (63). The calculations showed that equation (63) yielded values of $\Delta_{F,av}$ within $\pm 5\%$ of those computed

with equation (62), and that the associated overall weight uncertainty was less than ±1 percent of the total radiator weight in the cases of interest. Hence for the exploratory purposes of the present study, the use of equation (63) for $\Delta_{F,av}$ was thought to be acceptable and equation (63) was employed herein.

In the case of circumferential external fins the total fin weight is given by the formula

$$\begin{pmatrix}\text{External fin}\\ \text{weight}\end{pmatrix} = \rho_F \left[N \nu \pi(R_o^2 - R_a^2) \Delta_{F,av}\right] \begin{pmatrix}\text{Circumfer-}\\ \text{ential fins}\end{pmatrix} \quad (64)$$

with the number of fins per tube, ν , given by equation (44). As in the case of central-type external fins, the approximate value of $\Delta_{F,av}$ as given by equation (63) was employed for calculating the average fin thickness to be used in equation (64). Check calculations showed that, in the cases of interest, the uncertainty in weight arising from use of the approximate $\Delta_{F,av}$ was less than ± 1.5 percent of the total radiator weight; hence, use of equation (63) was thought to be acceptable and equation (63) was employed for the exploratory studies of circumferentially finned radiators.

Equations (58), (59), (60), and (61) or (64), define the weights of the radiator components. The radiator total weights presented in this report were computed by summing the weights of the indicated components. Auxiliary structure weight was not considered.

The radiator planform area was computed with the following formula, which allows for the incremental envelope area contributed by the headers, conservatively based on the largest occurring diameters of the supply and exhaust headers:

$$\left(\begin{matrix}\text{Planform}\\ \text{area}\end{matrix}\right) = \left[l + (d_{H,en} + 2\delta_{a,total}) + (d_{H,ex} + 2\delta_{a,total})\right] L_{H,unsplit} \qquad (65)$$

As indicated by equation (65), the header length involved in the planform area is not affected by whether or not the header is split.

GEOMETRIES INVESTIGATED

Tube Internal Geometries

Cross sections of the tube internal geometries investigated are presented in figure 3.

Figure 3a represents an internally unfinned tube, which serves as the reference geometry in the present study. The heat transfer and friction factor correlations employed for calculating this geometry are shown in figure 6; these correlations are taken from Reference 6. The parameters investigated for internally unfinned tubes are shown in Table 1.

Table 1. Geometries and Parameters Investigated

A. Radiators with central external fins:

Type of internal fin	None (figure 3a)	Short radial I & II (figure 3b)	Radially long, axially continuous (figure 3c)	Radially long, axially interrupted (figure 3d)
No. of internal fins per tube	-----	34 to 50	10 to 70	4 to 20
Internal fin thickness (inch)	-----	.004	.004	.004
Tube length (ft)	6 and 25	25	6 and 25	6 and 25
Tube i.d. (inch)	0.33 to 1.14	1.62 to 2.07	0.75 to 2.35	1.14 to 3.36
(Central blockage tube o.d.) / (Radiator tube i.d.)	-----	-----	0.20 and 0.25	0.20 and 0.25
Wall thickness of central blockage tube (inch)	-----	-----	.005	.005
External fin conductance parameter (N_{c,L_F})	0.2 to 1.0	1.0	0.3 to 1.0	0.3 to 1.0
No. of branches per header	1 and 2	1 and 2	1 and 2	1 and 2

(Table 1 continued next page)

Table 1. (Continued)

B. Radiators with circumferential external fins:

Type of internal fin	None (figure 3a)	Radially long, axially interrupted (figure 3d)
No. of internal fins per tube	-----	12
Internal fin thickness (inch)	-----	.004
Tube length (ft)	25	6
Tube i.d. (inch)	1.07	1.29
$\frac{\text{(Central blockage tube o.d.)}}{\text{(Radiator tube i.d.)}}$	-----	0.25
Wall thickness of central blockage tube (inch)	-----	.005
External fin-to-armor radius ratio (R_o/R_a)	4	4
External fin conductance parameter (N_{c,R_a})	.0045 to .049	.0045 to .049
No. of branches per header	2	2

Figure 3b represents tubes with short radial fins and no central flow blockage tube. The geometry labelled "Short Radial-II" provides more internal fin surface than does the geometry labelled "Short Radial-I". Figure 6 indicates that the same heat transfer and friction correlations were used for these internally finned tubes as were used for the internally bare geometry of figure 3a. The parameters investigated for tubes with short radial internal fins are summarized in Table 1.

Figure 3c represents tubes equipped with long radial fins and a central flow blockage tube. In the geometry of figure 3c the fins extend radially inward toward the tube center and stop at the surface of the flow blockage tube that prevents fluid from concentrating near the tube center. The heat transfer and friction correlations employed for the internally finned tubes of figure 3c are shown in figure 6; these correlations are taken from Reference 9. Table 1 lists the parameters evaluated for tubes with long radial internal fins and central flow blockage tube.

Figure 3d represents tubes equipped with axially interrupted radial fins. In a cross section perpendicular to the tube axis the fins resemble those of figure 3c, being long in the radial direction and stopping at the surface of a flow blockage tube. In a cross section parallel to the tube axis, however, the fins are interrupted at regular axial intervals and are rotated through an angle equal to half the wedge angle of the fins. The ratio of fin axial interruption interval-to-channel equivalent diameter employed was 1.2 ,

for which the heat transfer and friction data of Reference 10 were employed; these data are reproduced in figure 6. The parameters investigated for tubes with interrupted radial fins are listed in Table 1.

External Fin Geometries

Two types of external fins are considered herein, namely, central external fins and circumferential external fins.

Central-type external fins are shown schematically in figure 4. The characteristic dimensions of these fins are the transverse span, L_F, and the thickness, Δ_F. In the present study both L_F and Δ_F are dependent variables, and in the class of radiators investigated Δ_F decreases axially from entrance to exit stations of the tubes. Central external fins are the principal type considered in this report; such external fins are evaluated for all the internal geometries studied (figure 3 & Table 1A.)

Circumferential-type external fins are shown schematically in figure 5. For pre-computed armor radius (R_a) as discussed in the Calculation Procedure, the characteristic dimensions of circumferential fins are the outside radius, R_o, the axial spacing, s_F, and the thickness Δ_F. In the present study, both R_o and s_F are independent variables: for pre-computed R_a , the outside radius R_o is prescribed through the prescription $R_o/R_a = 4$; and the spacing s_F is varied parametrically through parametric variation of the conductance parameter N_{c,R_a}. The fin thickness, Δ_F , is a dependent variable; in the class

of radiators considered, Δ_F decreases axially from entrance to exit stations of the tubes, as discussed in the Calculation Procedure. Circumferential external fins are studied for two tube geometries, namely, 25-foot long internally unfinned tubes (figure 3a) and 6-foot long tubes with interrupted radial internal fins (figure 3d); see also Table 1B.

OPERATING CONDITIONS

All radiators studied were required to perform to the following specifications, which correspond to a solar powered Brayton cycle that delivers 10 KW of electrical power.

Fluid: Argon

Fluid flow rate: $\dot{m}$ = 2201.4 lb_m/hr = 0.6115 lb_m/sec

Fluid pressure at inlet to entrance header: 6.57 psia

Allowable ΔP for friction in entrance header, header-to-tube turning loss and tube entrance pressure losses: 0.15 psi

Fluid pressure after suffering tube entrance losses: 6.42 psia

In-tube ΔP: 0.30 psi

Pressure at tube exit plane: 6.12 psia

Allowable ΔP for tube exit losses, exhaust header friction and head losses: 0.12 psi

Fluid temperature at entrance to radiator tube, ignoring heat transfer in entrance header: 915 ^{o}R

Fluid temperature at exit from radiator tube: 536 ^{o}R

Fluid T_{av} in radiator: 725.5 ^{o}R

Assumed fluid film temperature in radiator: T_{film} = 705.7 ^{o}R

Assumed T_{av}/T_{film} : 1.028

Argon properties at T_{film} , based on Ref. 11 and kept constant for all radiators:

c_p = specific heat = 0.124 Btu/(lb_m ^{o}R)

μ = dynamic viscosity = 0.0666 lb_m/(hr ft)
= 18.5 x 10^{-6} lb_m/(sec ft)

k = thermal conductivity = 0.0127 Btu/(hr ft^2 ^{o}R ft^{-1})
= 3.528 x 10^{-6} Btu/(sec ft^2 ^{o}R ft^{-1})

Assumed material of armor, internal fins, external fins and headers: Aluminum of density 172 lb_m/ft^3 and thermal conductivity 110 Btu/(hr ft^2 ^{o}R ft^{-1})

Thickness of internal fin metal: .004 inch

Emissivity of armor coating: ϵ = 0.90

Armor zero penetration probability: P(0) = 0.90

Mission duration: 365 days

Effective environment temperature: T_e = 425 ^{o}R

RESULTS AND DISCUSSION

Weights and planform areas are presented for radiators that have internally unfinned tubes and for radiators that have internally finned tubes. The effects of tube diameter, tube length, number of internal fins per tube and external fin conductance parameter are indicated. Effects of splitting the supply and exhaust headers are shown. Possible effects of circumferential external fins are briefly considered. The weights presented are based on a total armor thickness that allows for the exposed surfaces of both the tubes and headers. The planform areas presented include the incremental envelope area contributed by the headers.

Internally Unfinned Radiators

The present section is concerned with internally unfinned radiators. Numerical results are given for radiators with 25-foot long tubes. The calculations showed that internally unfinned radiators with 6-foot long tubes are much larger and heavier than are 25-foot long radiators at the operating conditions considered.

Effect of tube diameter and of split headers: Figure 10 shows the effects of tube inside diameter, and of split headers, on the component and overall weights and on the planform area of internally unfinned radiators of 25 foot tube length. For all radiators in figure 10, the operating conditions listed on the preceding two pages of

the text apply; the external fins are of the central type (figure 4), and the conductance parameter, N_{c,L_F}, of the external fins is 1.0 at all axial stations of every radiator. The dashed lines in figure 10 correspond to radiators with unsplit headers, and the solid lines correspond to radiators with each header split into two branches (figure 2).

Figure 10 shows that if the tube inside diameter is increased while all other independent variables are kept fixed, then, in the range of tube diameters shown, each component weight varies one-directionally and the total weight passes through a minimum, as follows: As the tube diameter increases, the weight of the armored tubes decreases steadily, but with gradually diminishing slope; and the weights of the external fins and armored headers both increase steadily, the external fin weight increasing with continually increasing slope. The net effect of decreases in tube weight and increases in external fin and header weights is that the total radiator weight decreases to a minimum, and then increases again, as the tube diameter increases further.

Thus figure 10 shows that at fixed tube length and fixed radiator operating conditions, there exists a weight-optimum tube inside diameter.

Figure 10 indicates that for constant tube length, an increase in tube inside diameter results in an increase in radiator planform area.

Figure 10 also shows that the use of split headers results in reductions in radiator weight and planform area. The weight reduction results from decreases in the header diameters, header surface area, and surface area-dependent armor thickness when split headers are used. The small reduction in planform area is due to the decrease in the header diameters; it is recalled that the indicated planform areas include the projected areas of the supply and exhaust headers, conservatively based on the largest occurring diameters of those headers.

Effect of N_{c,L_F} : In figure 10, N_{c,L_F} is equal to 1.0 . The effects of variations in N_{c,L_F} are considered in this sub-section.

In studying the effects of N_{c,L_F} , a near-optimum radiator in figure 10 is chosen. This radiator has a tube length of 25 feet and a tube inside diameter of 1.07 inch, and employs split headers. At $N_{c,L_F} = 1$, the radiator weighs 972 lb or 97.2 lb/KW_e .

Figure 11 shows the effects of decreasing N_{c,L_F} alone, keeping constant the inside diameter, length and number of armored tubes. The figure shows that as N_{c,L_F} decreases, the weight of the external fins increases steadily, the header weight decreases steadily, and the armor weight decreases steadily but very slightly. The net effect of the changes in component weights is that the total radiator weight decreases slowly to a shallow minimum and then increases again. At $N_{c,L_F} = 0.3$, the radiator weight is 951 lb or 95.1 lb/KW_e .

Figure 11 shows that while the effect of N_{c,L_F} on radiator weight is small, its effect on planform area is substantial. Thus, as N_{c,L_F} decreases from 1.0 to 0.2, the planform area decreases steadily from about 700 to 500 ft^2. At $N_{c,L_F} = 0.3$, where the radiator weight is close to its minimum value, the planform area is 533 ft^2, including the small incremental area contributed by the headers. (For the case of 25 ft long tubes, the area contributed by the headers is only about 3 percent of the panel area. For the case of 6 ft long tubes, however, the header contribution to the planform area can be more than 10 percent of the panel area, as indicated later in the text during discussion of internally finned tubes.)

From the foregoing discussion, the optimum internally unfinned radiator of the present study has a specific weight of 95.1 lb/KW_e and a specific planform area of 53.3 ft^2/KW_e.

Comparison of the present results with those of an alternate study of internally unfinned Brayton cycle radiators: It is of interest to compare the results of this study with those of Reference 12, in which an independent analysis is made of Brayton cycle radiators that use a gas as the working fluid.

The optimum radiator of Reference 12 has a weight of 76.9 lb/KW_e and a planform area of 49.1 ft^2/KW_e . At operating conditions identical with those of Reference 12, the calculation procedure of the present study yields a radiator weight of 81.3 lb/KW_e at a planform area of 49.1 ft^2/KW_e . These values indicate that when

identical input data are employed, the calculation procedures of Reference 12 and of this study yield results that are in satisfactory agreement with each other. The 6 percent lower radiator weight of Reference 12 is believed to be due to the use of constant-thickness external fins in that Reference, as compared with axially tapered external fins in the present study.

Internally Finned Radiators

The effects of adding fin surface to the gas swept inner walls of the radiator tubes are discussed in the present section. Internal fin geometries of the sort shown in figure 3b to 3d are considered. The consequences of internal finning are examined from two viewpoints, as follows:

a) the effects of internal fins on the optimum values of the tube diameter, tube length, number of header branches, and conductance parameter of the external fins;

b) the effects of internal fins on radiator minimum weight and associated planform area.

Radiators equipped with central-type external fins are employed as the basis of discussion. Figures 12 to 20 present the numerical data from which the conclusions are drawn.

Effect of internal fins on optimum tube diameter: It was found from figure 10 for internally unfinned radiators that, for fixed tube length, there exists a tube diameter at which the radiator weight is a minimum. This is also true for internally finned radiators, as shown by figures 12a and 12b for tubes with short radial fins, by figure 13 for tubes with long radial fins, and by figure 14 for tubes with axially interrupted fins.

In figures 12 - 14, the radiator operating conditions, the tube length, the number of header branches and the value of N_{c,L_F} are the same as those for the internally bare radiators of figure 10. It is clear, therefore, that differences among the weight-optimum tube diameters in figures 10 - 14 are due to differences in the amounts and kinds of internal fin surface employed.

Comparison of figures 10 - 14 shows that the weight-optimum tube inside diameters of all four groups of internally finned radiators are larger than the 1.07 inch optimum value for the internally bare radiators of figure 10. This result indicates that if the tube length and all other relevant conditions are kept fixed, then, introduction of fins into the radiator tube results in an increase in the tube inside diameter for minimum weight. This increase in diameter results from the need to satisfy a fixed pressure drop requirement, in a tube of fixed length, when the friction surface per unit flow area in the tube interior increases.

From the viewpoint of radiator weight, an increase in tube diameter is undesirable, because it moves the armor radially outward and increases the armor weight even when the exposed surface area and wall thickness are fixed. However, the increase in tube inside diameter is not the only effect produced by the internal fins. These fins also contribute an increase in the gas heat transfer surface, and this produces a substantial increase in the overall heat transfer coefficient, U, with an attendant increase in the temperature of the tube wall. As a result of the rise in tube wall temperature, the amount of armor surface required to radiate the armor's share of the total heat load decreases significantly, and this tends to counteract the increase in tube diameter occasioned by the pressure drop requirement.

The net effect of the indicated opposing factors is that, for the geometries studied, the beneficial aspect of the internal fins prevails: the weights of the lightest internally finned radiators in figures 12 - 14 are noticeably lower than the weight of the lightest internally bare radiator of figure 10. The minimum weights in figures 12 - 14 are not optimum for internally finned radiators because the 25 ft tube length underlying those figures is considerably off-optimum for tubes with internal fins.

To the extent that reductions in tube inside diameter produce reductions in the weight of the armor, decreases in tube diameter are desirable. Such decreases can be achieved for internally finned tubes by reducing the tube length. This is shown by figures 15 and 16 for

radiators in which the tubes are 6 feet long. In figures 15 and 16, the tube inside diameters for minimum radiator weight are significantly smaller than the analogous ones in figures 13 and 14; the weight-optimum diameters (1.23 and 1.29 inches) for the 6 ft long internally finned tubes are only moderately larger than the 1.07 inch value which is optimum for the 25 ft long internally unfinned radiator of figure 10.

From the viewpoint of reductions in tube wall weight by reductions in tube inside diameter, it is of interest to compare the weights of the tube walls in figure 13 with those in figure 15, and also the wall weights in figure 14 with those in figure 16. Such comparisons show that for the range of tube inside diameters involved in those figures, reductions in tube diameter do produce significant decreases in tube wall weight. It is noteworthy, however, that the large decreases in tube diameter are accompanied by substantial increases in header weight. Possible methods of reducing header weight are noted later in the text.

The foregoing discussion has indicated the following:

If the tube length is fixed by considerations other than radiator performance and is required to have the same value regardless of tube internal geometry, then the weight-optimum tube diameter of internally finned tubes will be larger than that of internally bare tubes, the magnitude of the difference in optimum diameters being dependent on the kind and amount of internal surface employed. The larger diameter of the internally finned tubes would tend to reduce, but not nullify, the gains inherent in the increased

armor temperature that occurs when internal fins are used.

On the other hand, if the tube length can be freely modified to optimize radiator weight, then the weight-optimum tube i.d. for internally finned tubes can be maintained, if desired, at values that differ only moderately from the optimum i.d. of internally bare tubes, by reductions in the tube length.

Effect of internal fins on optimum tube length: From the foregoing discussion it follows that the optimum length of internally finned tubes is shorter than the optimum length of internally bare tubes. This is numerically substantiated later in the text, by comparing minimum-weight internally finned radiators of 6 ft tube length with the optimized internally bare radiator of 25 ft tube length.

Effect of internal fins on optimum number of header branches: Reductions in the length and weight-optimum diameter of internally finned tubes results in a substantial increase in the required number of tubes. This, in turn, leads to substantial increases in the length, diameters and weights of the headers. The increases in number of tubes and in header weight may be seen by comparing values for the lightest radiators in figures 14 and 16. A comparison is shown in Table 2.

Table 2. Effect of Tube Length on Optimum Tube Diameter, Number of Tubes and Header Weights

Figure	Tube length (ft)	Internal fins per tube	Tube i.d. for min. rad'r wt. (inch)	No. of tubes* (to nearest integer)	Header weight** (lb)
14	25	8	2.98	12	62
16	6	12	1.29	63	328

*Not shown in figures 14 and 16.

**$N_c, L_F = 1.0$.

The table shows clearly the need for provisions to reduce header weight when reductions are made in tube length and diameter.

Two independent variables that influence strongly the weight of the headers are (1) the number of branches into which each header is split, and (2) the conductance parameter (N_{c,L_F}) of the external fins, which governs the span of those fins. The header weights in the table correspond to supply and exhaust headers each split into two branches (figure 2) and to $N_{c,L_F} = 1.0$. These values of the two independent variables are not optimum for the 6 ft long radiator of the foregoing table. The present sub-section is concerned with the effect of internal fins on the optimum number of branches into which the headers may be split.

Comparison of the weights of split and unsplit headers in figures 10,11, 12 and 15 shows that for both 25 ft long and 6 ft long tubular radiators, the effect of splitting the headers once is to produce about a 30 percent reduction in the header weight. This magnitude of weight reduction can be shown to be repeated if each branch is divided into two sub-branches. The reason for the large weight decrease produced by subdividing the headers is that each time a header or branch is split, the path length of fluid is halved. Thus the diameter of the duct can be reduced without increasing the fluid pressure drop. The reduction in header diameter accounts for the reduction in header weight.

As feed and drain lines are required at the junctions of the header branches, and as the weights of these lines increase when

the number of branches increases, there is a point beyond which the number of header subdivisions cannot be profitably increased. This is particularly true if the lines that drain (or feed) the branch junctions have to be armored against penetration by meteoroids. For the 25 ft long internally finned tubular radiator of the foregoing table, in which the once-split headers weigh only 62 lb, or for the 25 ft long optimum internally bare radiator with a split header weight of 135 lb (figure 10), additional sub-division of the headers would yield at best small additional reductions in radiator weight. For the 6 ft long internally finned tubular radiators of the foregoing table, however, in which the once-split headers still weigh 328 lb, further subdivision of the headers would appear to be desirable.

The foregoing discussion indicates that the effect of internal finning of the radiator tubes is to increase the optimum number of branches into which the supply and exhaust headers are split. The optimum number of branches is that value which yields the lowest combined weight of the headers and their feed and drain lines; a secondary factor in determining the optimum number of header branches is the reduction in armor weight resulting from the decrease in the exposed header surface as the diameters of the headers decrease.

Effect of internal fins on optimum N_{c,L_F}: At pre-computed values of tube o.d. and $(dQ)/(dQ_b^*)$ as described in the Calculation Procedure, the conductance parameter N_{c,L_F} controls the span of the external

fins. Thereby it affects the weight not only of the external fins, but also of the headers and armored tubes (through the dependence of the final armor thickness on the exposed surface of the headers), and also affects significantly the radiator planform area.

The effects of N_{c,L_F} on the component and overall weights and on the planform area of internally bare radiators were indicated in figure 11. In figure 11 it was found that because variations in N_{c,L_F} produce changes in external fin weight that differ in direction from the changes in header and armored tube weights, there exists an optimum value of N_{c,L_F}. For the internally unfinned radiator of figure 11, the optimum N_{c,L_F} was about 0.30 . The effect of internal finning of the radiator tubes on the optimum value of N_{c,L_F} is considered in the present sub-section.

The effects of N_{c,L_F} on the component and overall weights and on the planform areas of internally finned radiators are shown in figures 17 - 20. Figures 17 and 18 correspond to radiators with 25 ft long tubes, and figures 19 and 20 correspond to radiators with 6 ft long tubes. In figures 17 and 19 the internal fins are radially long, as shown in figure 3c; in figures 18 and 20 the internal fins are radially long and axially interrupted, as shown in figure 3d. In all cases the supply and exhaust headers are each split once.

Figures 17 - 20 show that the effects of N_{c,L_F} on the component weights and on the planform area of internally finned radiators are similar to those in unfinned radiators; and that in all cases N_{c,L_F} either possesses or approaches a weight-optimum value in the range of N_{c,L_F} considered.

Figures 17 and 18 show that for the 25 ft long internally finned radiators, the effect of N_{c,L_F} on total radiator weight is small in the range of N_{c,L_F} considered; this was also true for the 25 ft long internally bare radiators of figure 11. Careful comparison of figures 17 and 18 with figure 11 discloses, however, that the N_{c,L_F} for minimum weight of the 25 ft long internally finned tubes is substantially higher than the 0.3 weight-minimum value of N_{c,L_F} for the internally bare radiators of figure 11. The change in weight-optimum N_{c,L_F} is due to the substantially larger diameters of the internally finned tubes, as shown for the 25 ft long radiators in Table 3, below. Increases in tube diameter, with attendant decreases in the number of tubes and in the length and weight of the headers, cause the headers to become lighter than the external fins (or alternately, cause the external fins to become heavier than the headers). Since increases in N_{c,L_F} produce decreases in external fin weight, the weight-optimum value of N_{c,L_F} moves toward higher values as the tube diameter increases. Thus, at fixed tube length, the effect of internal fins is to increase the weight-optimum value of N_{c,L_F}, in comparison with the best value for internally bare tubes.

Table 3. Tube Lengths and Diameters In Several Minimum-Weight Radiators

Figure	Tube length (ft)	No. of internal fins per tube	Tube i.d. (inch)	Tube o.d. (inch)
11	25	None	1.07	1.48
17	25	10	2.05	2.44
18	25	8	2.98	3.39
19	6	30	1.23	1.63
20	6	12	1.29	1.68
↓	↓	20	1.48	1.87

On the other hand, figures 19 and 20 show that if the weight-optimum tube diameter of internally finned radiators is reduced by reducing the tube length to 6 ft (Table 3), the header weight dominates over the external fin weight. Thus, to achieve minimum radiator weight, N_{c,L_F} must decrease to values lower than those that are optimum for internally finned radiators with 25 ft long tubes. In figures 19 and 20, the weight-optimum values of N_{c,L_F} are all close to the 0.30 value which was previously found to be optimum for 25 ft long internally bare radiators.

The foregoing discussion indicates that internal finning of the radiator tubes results in a marked tendency of the weight-optimum N_{c,L_F} to increase. The discussion also shows, however, that if the optimum diameters of internally finned tubes are reduced by means of reductions in the tube length, the weight-optimum N_{c,L_F} can be maintained at a low value, with substantial attendant benefits in radiator weight and planform area.

In figures 17 - 20, explicit note may be taken that reductions in N_{c,L_F} produce decreases in the weights of the headers. Reductions in N_{c,L_F}, together with optimization of the number of header branches as discussed earlier in the text, are two effective means for reducing header weight.

Existence of optimum number of internal fins per tube: For internally finned radiator tubes it is desirable to inquire whether there exists an optimum number of fins per tube. This question may be discussed by use of figures 15, 16 and 20. Figure 15 corresponds to 6 ft long tubes with radially long internal fins (figure 3c), and figures 16 and 20 correspond to 6 ft long tubes with radially long-and-axially interrupted internal fins (figure 3d).

Figure 15 shows that at each of two different numbers of internal fins per tube (20 and 30), a weight-optimum tube i.d. occurs, and that the optimum i.d. of the tubes with 30 internal fins is noticeably larger than the optimum i.d. of the tubes with 20 internal fins. (The growth in weight-optimum tube diameter with increases in the amount of internal fin surface has been discussed previously in the text.) In addition, figure 15 shows that the minimum-weight radiator with 30 fins per tube is lighter, and has a significantly smaller planform area, than the minimum-weight radiator with 20 fins per tube.

Thus figure 15 shows that one number of internal fins can be better than another from the viewpoints of both radiator weight and size.

On the other hand, figure 16 shows that for an internal fin geometry which differs from that of figure 15, three different internal fin numbers per tube (12, 16 and 20), yield respective minimum radiator weights that are indistinguishable from one another. The planform areas, however, are not all the same; the planform area decreases as the number of internal fins per tube increases. Thus, one number of internal fins may be better than another number from the viewpoint of radiator size. It can be shown as follows, however, that even in a range where significant changes in the internal fin surface per tube appear to produce no effect on radiator weight, there does exist a weight-optimum number of internal fins per tube:

It is noted that for all the radiators of figure 16, N_{c,L_F} is equal to 1.0 . The discussion in the foregoing sub-section has shown that the weight-optimum N_{c,L_F} changes as the tube diameter changes. This indicates that N_{c,L_F} can be used to identify the weight-optimum number of internal fins per tube, as illustrated by figure 20. Figure 20 shows that when optimized with respect to N_{c,L_F} as well as with respect to tube i.d. (figure 16), the minimum-weight radiator with 12 internal fins per tube is lighter than the minimum-weight radiator with 20 fins per tube. The radiator with the larger number of internal fins per tube remains the smaller in planform area, however, at all values of N_{c,L_F} in the range shown in figure 20.

The foregoing discussion indicates that for each type of internal fin geometry there exists a weight-optimum number of internal fins per tube. At each prescribed set of radiator operating conditions and tube length, the optimum fin number per tube may be identified by parametric exploration of that fin number, and by optimization of both the tube i.d. and N_{c,L_F} at each assigned value of internal fins per tube.

Minimum-weight internally finned radiators: For internally finned radiators with central-type external fins, the minimum specific weights and associated specific planform areas computed in the present study were as follows:

Table 4. Minimum Weight Internally Finned Radiators With Central External Fins

Tube length (ft)	Internal fin type	No. of fins per tube	Radiator sp. wt. (lb/KW_e)	Sp. planform area (incl. headers) (ft^2/KW_e)
25	Long radial (figure 3c)	10	83.3	45.7
6	Long radial (figure 3c)	30	82.1	33.7
6	Interrupted (figure 3d)	12	78.4	33.0

The headers of the radiators in the foregoing table are split once. In the case of the radiator of 25 ft tube length, the combined weight of the supply and exhaust headers is 73 lb, hence only small

gains could be achieved by further header subdivision. In the case of each radiator of 6 ft length, however, the header weight is about 225 lb. For the radiators of 6 ft tube length, subdivision of each header into 4 branches (instead of the 2 branches that underlie the above-tabulated radiator weights) would reduce the header weights by about 70 lb, and the radiator specific weights by about 7 lb/KW_e.

The planform areas in the foregoing table include the incremental projected areas contributed by the headers, conservatively based on the largest occurring header diameters. In the case of the radiator with 25 ft long tubes, the header area contribution is only about 3 percent of the basic panel area of the tubes plus their external fins. In the case of the radiators with 6 ft long tubes, however, the header area contribution is about 13 percent of the tube-fin panel area. Inasmuch as the headers and tube-fin panel must be housed in the same vehicle, it appears reasonable to include the header area in the total (projected) planform area.

The radiator specific weights and sizes in the foregoing table may be compared with the 95.1 lb/KW_e and 53.3 ft^2/KW_e of the optimum internally unfinned radiator of the present study. Such comparison shows that for the class of radiators and operating conditions considered, internal finning of the tubes results in weight reductions of 12 to 18 percent, and size reductions of 14 to 38 percent, in comparison with the weight and size of the optimum radiator with

internally unfinned tubes. If the headers of the lighest internally finned radiator in the foregoing table were split twice instead of once, that radiator would be about 25 percent lighter and about 40 percent smaller than the optimum internally unfinned radiator of the present study.

Radiators With Circumferential External Fins

The parts of the external fins that are distant from the surface of the tubes depend upon conduction for most of the heat that reaches them. Hence there is a substantial temperature decrease along the fins in the direction away from the tube surface. In the case of central-type external fins, the average temperature of the body of the fin in the neighborhood of the supply header is lower than the temperature of the header. In that region of the radiator, the fins and the fin-to-tube junctions are subject to tensile stress. Similar stress may exist in the neighborhood of the exhaust header. In a radiator with non-isothermal working fluid, there is also a temperature decrease in all metal parts in the direction of fluid flow. In the case of central-type fins that are continuous, constrained plate-type deformation or stress may arise from the simultaneously occurring axial and transverse temperature fields. Thus, radiators with central-type external fins may operate with substantial stress at the fin-to-tube junctions or in the body of the fins. These stresses are probably of greater significance than those that exist in the tube walls as a result of circumferential temperature non-uniformity in centrally-finned tubes.

In the case of circumferential, i.e., annulus shaped, external fins (figure 5), the radial temperature drop in the fins that arises from outward conduction of heat leads to a compression of the fins at their junctions with the tubes. Under compressive force, separation between fin and tube appears unlikely. In addition, when each fin is a separate unit, temperature differences between fin and header, or between one fin and another, do not give rise to fin-to-tube junction stress or to added stress within the body of the fin. Further, with a circumferential arrangement of the fins, the temperature in the tube wall tends to be uniform around the circumference. Thus, radiators with circumferential external fins may be significantly less vulnerable to thermal stress than are radiators with central-type external fins.

Circumferentially finned tubes also appear to offer relative ease of fabrication; and the fins themselves may perform a non-negligible bumper function against obliquely arriving meteoroids and thereby may permit reduction in the thickness of the armor.

Accordingly, it is of interest to make exploratory calculations of the sizes and weights of tubular radiators equipped with circumferential external fins. Results of preliminary calculations for such radiators are presented in figure 21.

Figure 21 presents calculated weights and planform areas for two sets of radiators equipped with circumferential fins of radius ratio $R_o/R_a = 4$, with the fins of adjacent tubes just touching each other. One set of curves in figure 21 corresponds to the internally unfinned radiator of 25 ft tube length and 1.07 inch tube i.d. that

was previously optimized in figures 10 and 11. The second set of curves corresponds to the internally finned radiator of 6 ft tube length and 1.29 inch tube i.d. with 12 axially interrupted internal fins per tube that was previously optimized in figures 16 and 20.

The two sets of radiators in figure 21 have the following properties:

(a) For each set of radiators, the number of tubes, the tube length and the tube inside and outside diameters are the same for the circumferentially finned geometry as they were for the centrally finned geometry. Hence, for each set of radiators the armored tube weight is constant and equal to the tube weight in the centrally finned geometry.

(b) For each set of radiators, the header lengths and weights and the radiator planform area are constant. This follows from the fact that the number of tubes, the tube outer diameter, the ratio R_o/R_a and the lateral spacing between tubes are all constant.

(c) The overall convection-conduction coefficient U , the armor temperatures, and hence also the ratio $(dQ)/(dQ_b^*)$, are the same for the circumferentially finned radiators as for the centrally finned radiators. That is, each set of radiators has a fixed combination of values of D_a (or R_a), R_o/R_a , and $(dQ)/(dQ_b^*)$. Therefore, as was discussed in the Calculation Procedure, parametric variation of N_{c,R_a} is equivalent to parametric variation of the fin axial spacing (s_F). In addition, as N_{c,R_a} is varied, the fin thickness (Δ_F) varies in accordance with equation (43) of the Calculation Procedure. Hence, parametric variation of N_{c,R_a} implies definite variations in the spacing, thickness and axial pitch ($s_F + \Delta_F$) of the external fins, under the conditions governing figure 21.

It follows from the foregoing that N_{c,R_a} is the only independent variable in figure 21, and that the radiator weight variations in the figure are due entirely to variations in the weight of the external fins.

Figure 21 shows that as N_{c,R_a} increases from an initially low value, the axial pitch between fins decreases steadily. Since the tube length is fixed, a decrease in fin axial pitch implies an increase in the number of fins per tube. With increases in N_{c,R_a}, however, the fin thickness (not shown separately in figure 21) decreases steadily. The balance between the increase in the number of fins and decrease in their thickness leads to a minimum in the weight of the fins at an intermediate value of N_{c,R_a}; in figure 21, the value of N_{c,R_a} at which the minimum fin weight occurs is .03 for both sets of radiators shown in the figure. Since the fins are the only component that can affect the total radiator weight under the conditions of figure 21, the radiator weights also have their minimum values at $N_{c,R_a} = .03$. The following table presents data of interest for the minimum weight radiators of figure 21.

Table 5. Minimum Weight Radiators With Circumferential External Fins

Tube length (ft)	Internal fin type	Internal fins per tube	Radiator sp. wt. (lb/KW_e)	Sp. planform area (incl. headers) (ft^2/KW_e)
6	Interrupted (figure 3d)	12	81.6	23.1
25	None	None	102.5	36.8

The values in Table 5 make no allowance for mutual shadowing of the finned tubes, nor for possible weight reductions due to the bumper effect of the circumferential external fins. The values in Table 5 are, therefore, only tentative. Thus, tentatively, the table shows that the internally finned radiator of 6 ft tube length is about 20 percent lighter and more than 35 percent smaller than the optimum internally unfinned radiator of 25 ft tube length. These percentages are substantially the same as the corresponding ones for centrally finned radiators.

A comparison between the minimum-weight internally finned radiators of 6 ft tube length in Tables 4 and 5 indicates, tentatively, that the radiator with circumferential external fins is about 5 percent heavier and about 30 percent smaller than the radiator with central-type external fins.

Comparison of weights and sizes also indicates, tentatively, that the minimum weight internally finned radiator of 6 ft tube length with circumferential external fins is about 15 percent lighter and about 55 percent smaller than the optimum internally unfinned radiator of 25 ft tube length equipped with central-type external fins.

CONCLUDING REMARKS

A preliminary study has been made of Brayton cycle radiators that use a gas as their working fluid. The radiators have been assumed to be assemblies of armored, externally finned tubes that lie in one plane and radiate heat to both sides of the plane. The radiator operating conditions that have been assumed correspond to a solar-powered Brayton cycle that uses argon as working fluid and delivers 10 kilowatts of electrical power steadily during a 365 day mission, in an environment in which protection against meteoroids is a substantial requirement.

One purpose of the study was to develop a method of calculating the sizes and weights of radiators of the sort described in the preceding paragraph. A method of calculating such radiators has been presented.

Another purpose of the study was to determine whether significant effects on radiator size and weight result from the use of finned heat transfer surface inside the radiator tubes. For this purpose, four internal fin geometries have been evaluated in radiators equipped with conventional central-type external fins.

A third purpose of the study was to consider briefly the effects on radiator size, weight and stress that might result from the use of circumferential (annular) radiating fins on the external surfaces of the radiator tubes. Illustrative results for radiators equipped with circumferential external fins have been presented.

The principal findings of the study are as follows:

(a) The main effect of internal fins is to reduce substantially the radiator planform area; to a lesser but non-negligible extent, internal fins also reduce the radiator weight. The numerical results indicate that optimized radiators with internal fins can be more than 35 percent smaller in size and more than 15 percent lighter in weight than optimized radiators without internal fins.

(b) Circumferential external fins may offer relative ease of fabrication, relative freedom from thermal stress, and a bumper effect against obliquely approaching meteoroids. If tube-to-tube occlusion does not necessitate wide spacing between tubes, circumferential external fins may offer worthwhile reductions in radiator size. With occlusion neglected, a 30 percent reduction in planform area was computed on substituting circumferential for central-type external fins in the smallest (internally finned) radiator studied.

As part of the study leading to the foregoing findings, the following were done:

The numerical results were employed to demonstrate that there exist optimum values for the independent geometric variables of the radiator, namely, tube length, tube inside diameter, number of internal fins per tube for each species of internal fin geometry, and number of branches into which the headers are split. It was also indicated that an optimum value exists for the conductance parameter of the external fins, and that the optimum value is affected by the diameter of the tube.

The effects of internal fins on the weight-optimum values of the independent geometric variables were discussed. It was indicated that

(1) The weight-optimum length of internally finned tubes is shorter than that of internally unfinned tubes .

(2) At fixed tube length, the weight-optimum diameter of internally finned tubes is larger than that of internally bare tubes; but if a relatively short length is used for internally finned tubes, then the weight-optimum diameter is about the same as that of internally bare tubes.

(3) If a relatively short tube length and associated optimum inside diameter of internally finned tubes are both used, the optimum value of the conductance parameter for the external fins is about the same for both internally finned and internally bare tubes.

(4) The optimum number of header subdivisions is significantly larger for internally finned radiators than for internally bare radiators.

APPENDIX A

Symbols

A	flow area, ft^2
a	correction factor for finite plate thickness and for spalling, 1.75, non-dimensional
b	radial length of internal fin, ft
C_a	coefficient in armor thickness equation, $ft^{0.502}$
C_T	temperature coefficient, non-dimensional
c	speed of sound in armor material, ft/sec
c_p	specific heat at constant pressure, $Btu/lb_m\ ^oR$
D	outside diameter, ft
d	inside diameter, ft
dQ	heat radiated by an infinitesimal surface element, consisting of armor surface-plus-external fin surface, in an externally finned radiator, Btu/hr
dQ_b	heat radiated by an infinitesimal element of bare armor surface in an externally unfinned radiator, Btu/hr
dQ_b^*	heat radiated by an infinitesimal element of bare armor that has the same surface area and the same surface temperature as the armor of the externally finned element which radiates heat dQ defined above. The numerical value of dQ_b^* is equal to $\sigma\epsilon\ (T_{a,x}^4 - T_e^4)\ dS_a$, in which ϵ, $T_{a,x}$, T_e and dS_a are the same as those of the armor surface in the externally finned element which radiates the heat dQ defined above, Btu/hr
E	modulus of elasticity, lb_f/ft^2
f	friction factor, non-dimensional
G	mass flow rate per unit flow area, $lb_m/hr\ ft^2$
g	gravitational conversion factor, $32.2 \times (3600)^2$, $(lb_m/lb_f)(ft/hr^2)$; in eq. (25), $g = 32.2\ (lb_m/lb_f)(ft/sec^2)$
h	convective heat transfer coefficient of gas, $Btu/hr\ ft^2\ ^oR$

k	thermal conductivity, Btu/hr ft^2 ^oR ft^{-1}
L	length, ft
ℓ	length of radiator tube, ft
$\dot{m}$	mass flow rate, lb_m/hr
N	number of radiator tubes, non-dimensional
N_c	black body conduction parameter of external fin, non-dimensional
N_{c,L_F}	N_c based on fin length, $2\sigma T_a^3 L_F^2/k_F \Delta_F$, non-dimensional
N_{c,R_a}	N_c based on armor radius (inside radius of circumferential fin), $2\sigma T_a^3 R_a^2/k_F \Delta_F$, non-dimensional
n	number of internal fins per tube; also, half the number of branches of a header split into 2n branches, non-dimensional
Pr	Prandtl number, non-dimensional
P_w	wetted perimeter, ft
$P(0)$	zero penetration probability, non-dimensional
p	static pressure, lb_f/ft^2
Q	total heat release; heat release of externally finned radiator, Btu/hr
q	heat released by a single tube, Btu/hr
R	radius, ft
r	tube inside radius, ft; also, thermal resistance, $^oR/(Btu/hr)$
Re	Reynolds number, non-dimensional
S	surface area, ft^2
s	axial spacing of circumferential external fins, ft
T	temperature, ^oR
U	heat transfer coefficient referred to outer surface of armor, Btu/hr ft^2 ^oR
$\bar{V}$	mean speed of meteoroids, ft/sec
v	gas speed, ft/hr
x	distance from radiator tube entrance plane; or from entrance plane of supply header, ft

Greek symbols:

α	meteoroid mass distribution constant, 5.3×10^{-11} gm$^{\beta}$/ft^2-day
β	meteoroid mass distribution constant, 1.34, non-dimensional
Δ	thickness of external fin, ft; drop (in pressure)
δ	thickness of armor or internal fin, ft
ϵ	emissivity, non-dimensional
η	efficiency, effectiveness, non-dimensional
θ	exponent on the speed ratio $\overline{V}/c$, non-dimensional
μ	dynamic viscosity, lb_m/hr ft
ν	number of circumferential external fins per tube, non-dimensional
ρ	mass density, lb_m/ft^3
σ	Stefan-Boltzman constant, 0.171×10^{-8} Btu/hr ft^2 $^oR^4$
τ	time, days

Subscripts:

a	armor
av	average
b	bare armor radiator
e	environment
eff	effective
en	entrance station
eq	equivalent
ex	exit station
F	external fin

f	internal fin
film	fluid film
flow	flow area
fr	friction
g	gas
H	header
i	inside; inner surface of tube
L_F	based on length of external fin
momentum	arising from change in fluid momentum
o	outside
p	particle (meteoroid)
R_a	based on armor radius
split	relating to headers split into two or more branches
t	target
total	based on combined contributions of armored tubes and headers
tube	pertaining to radiator tube
unsplit	relating to unsplit header
w	wall; wetted
x	at a station distant x from radiator tube entrance plane, or from supply header entrance plane; also, "up to station x" when applied to armor surface ($S_{a,x}$)

APPENDIX B

DERIVATION OF ARMOR THERMAL RELATIONS

The relations presented in the text for U, $T_{a,x}$ and $S_{a,x}$, equations (28), (30) and (34), respectively, are derived in the present appendix. For this purpose a representative tube like the one shown in figure 22 is considered. Figure 22 shows tube internal details representative of those considered in this study, but gives no details of external fins that would normally be present on the outer surface of the armor. The external fins are taken into account on a generalized basis by the parameter $(dQ)/(dQ_b^*)$. This parameter encompasses a large variety of external fin geometries without need for detailed specification of those geometries.

Derivation of the expression for U: Heat balances, expressed in terms of component and overall resistances to heat flow, are employed.

Steady state, one-dimensional heat flow is assumed. The inner and outer wall temperatures of the tube are assumed to be circumferentially uniform, and the temperature of the gas within the tube is assumed to be uniform over the cross section of the tube. Heat flow from the gas to the outer surface of the armor in the length interval (x, dx) is considered.

The resistance to heat flow from the gas to the inner wall of the tube is expressible as

$$r_{g,x} = \frac{T_{g,x} - T_{i,x}}{dQ} \tag{B1}$$

In equation (B1), $r_{g,x}$ includes the resistance to heat flow from the gas to the fins. The quantity $T_{i,x}$ is the temperature of the inner wall of the tube proper. For thin fins, the fin bases and their exposed sides are considered to be part of the inner wall of the tube and are assumed to be at the same temperature $T_{i,x}$ as the tube inner wall.

The expression for $r_{g,x}$ in terms of the gas heat transfer coefficient and the effective heat transfer surface is

$$r_{g,x} = \frac{1}{h\, dS_{eff}} \tag{B2}$$

in which dS_{eff} is the element of effective heat transfer surface swept by the gas. The formula for dS_{eff} is as follows:

$$\left.\begin{aligned} dS_{eff} &= dS_{w,i} + \eta_f\, dS_f \\ &= \left(1 + \eta_f \frac{dS_f}{dS_{w,i}}\right) dS_{w,i} \\ &= \left(1 + \eta_f \frac{S_f}{S_{w,i}}\right) dS_{w,i} \end{aligned}\right\} \tag{B3}$$

The term $dS_{w,i}$ consists of the sum of the exposed portion of the tube inner wall, the exposed portion of the inner surfaces of the fin bases, and the exposed sides of the fin bases. For fins as shown in figure 22, the exposed portion of the inner wall of a single tube is given by

$$\begin{pmatrix}\text{Exposed portion of}\\ \text{inner wall, per tube}\end{pmatrix} = \left(\frac{1}{2}\,\pi\, d_i\right) dx$$

The exposed inner surface of the fin bases, taking account of the portions covered by the roots of n fins, each of thickness δ_f, is given for a single tube by the expression

$$\begin{pmatrix}\text{Exposed inner}\\ \text{surface of fin}\\ \text{bases, per tube}\end{pmatrix} = \left[\frac{\pi}{2}(d_i - 2\,\delta_f) - n\,\delta_f\right] dx$$

The surface exposed by the sides of the fin bases, taking into account that there is one exposed side per fin, is given by

$$\begin{pmatrix}\text{Surface exposed}\\ \text{by sides of fin}\\ \text{bases, per tube}\end{pmatrix} = (n\,\delta_f)dx$$

The quantity $dS_{w,i}$ is obtained by summing the three foregoing components of the exposed inner surface per tube, and multiplying by the number of tubes; thus, $dS_{w,i}$ is given by the following expression:

$$dS_{w,i} = \pi (d_i - \delta_f) N\, dx$$
$$= \pi\, d_i\, N\, dx \left(1 - \frac{\delta_f}{d_i}\right) \tag{B4}$$

Define

$$dS_{tube} \equiv \pi\, d_i\, N\, dx \tag{B5}$$

$$h_{eff} \equiv h \left(1 + \eta_f \frac{S_f}{S_{w,i}}\right) \tag{B6}$$

With these definitions, the term $h\, dS_{eff}$ becomes

$$h\, dS_{eff} = h_{eff} \left(1 - \frac{\delta_f}{d_i}\right) dS_{tube} \tag{B7}$$

and the equation for the local thermal resistance of the gas becomes

$$r_{g,x} = \frac{T_{g,x} - T_{i,x}}{dQ} = \frac{1}{h_{eff} \left(1 - \frac{\delta_f}{d_i}\right) dS_{tube}} \tag{B8}$$

The heat flow by one-dimensional conduction across the wall of a single armored tube is given by (Ref. 13)

$$\left.\begin{aligned} dq &= \frac{2\pi\, k_a\, (dx)\, (T_{i,x} - T_{a,x})}{\ln\left(\frac{D_a}{d_i}\right)} \\ &\equiv \frac{2(\pi\, D_a\, dx)\, k_a\, (T_{i,x} - T_{a,x})}{D_a \ln\left(\frac{D_a}{d_i}\right)} \end{aligned}\right\} \qquad \text{(B9)}$$

For N identical tubes the total heat flow is

$$\left.\begin{aligned} dQ = N\, dq &= \frac{2(N\pi\, D_a\, dx)\, k_a\, (T_{i,x} - T_{a,x})}{D_a \ln\left(\frac{D_a}{d_i}\right)} \\ &= \frac{2(dS_a) k_a\, (T_{i,x} - T_{a,x})}{D_a \ln\left(\frac{D_a}{d_i}\right)} \end{aligned}\right\} \qquad \text{(B10)}$$

The resistance to heat flow across the armor is then

$$r_{a,x} = \frac{T_{i,x} - T_{a,x}}{dQ} = \frac{D_a \ln (D_a/d_i)}{2k_a\, dS_a} \qquad \text{(B11)}$$

The total resistance to heat flow from the gas to the outer surface of the armor is the sum of the resistances of the gas and of the armor; thus,

$$r_x = r_{g,x} + r_{a,x} \tag{B12}$$

Combining the expressions in equations (B8) and (B11), and using the fact that

$$\frac{dS_a}{dS_{tube}} = \frac{D_a}{d_i}$$

equation (B12) takes the form

$$r_x = \frac{1}{h_{eff}\left(1 - \frac{\delta_f}{d_i}\right)} \frac{1}{dS_a} \left[\frac{D_a}{d_i} + h_{eff}\left(1 - \frac{\delta_f}{d_i}\right) \frac{D_a}{2k_a} \ln\left(\frac{D_a}{d_i}\right) \right] \tag{B13}$$

Also, again by summation of equations (B8) and (B11),

$$r_x = \frac{T_{g,x} - T_{a,x}}{dQ} \tag{B14}$$

Equating the right members of (B13) and (B14) and solving for dQ,

$$dQ = \frac{h_{eff}\left(1 - \frac{\delta_f}{d_i}\right)\left(T_{g,x} - T_{a,x}\right) dS_a}{\frac{D_a}{d_i} + h_{eff}\left(1 - \frac{\delta_f}{d_i}\right)\frac{D_a}{2k_a} \ln\left(\frac{D_a}{d_i}\right)} \qquad (B15)$$

Equation (B15) may be simplified by writing

$$dQ = U\left(T_{g,x} - T_{a,x}\right) dS_a \qquad (B16)$$

which is a defining equation for U. Comparing equations (B15) and (B16), the expression for U is

$$U = \frac{h_{eff}\left(1 - \frac{\delta_f}{d_i}\right)}{\frac{D_a}{d_i} + h_{eff}\left(1 - \frac{\delta_f}{d_i}\right)\frac{D_a}{2k_a} \ln\left(\frac{D_a}{d_i}\right)} \qquad (B17)$$

which is the formula for U in equation (28) of the text.

Derivation of equation for armor temperature: The expression for the local armor temperature as given by equation (30) of the text is derived in the present sub-section. The derivation makes use of

the ratio $(dQ)/(dQ_b^*)$. In this ratio, dQ is the total heat radiated by an element of armor surface and its external fins, the local temperature of the armor surface being $T_{a,x}$; the term dQ_b^* is the heat that would be radiated by the same armor surface element if the external fins were removed and the surface temperature of the armor were somehow maintained at $T_{a,x}$.

By identity,

$$(dQ)_x = \frac{(dQ)_x}{(dQ_b^*)_x} \quad (dQ_b^*)_x \tag{B18}$$

The appearance of the subscript x in equation (B18) signifies that dQ and dQ_b^* both change with x. In the general case, $(dQ)_x/(dQ_b^*)_x$ will also change with x.

For a surface element of bare armor operating steadily at temperature $T_{a,x}$ in an environment of effective temperature T_e, the net heat lost by radiation is given by

$$(dQ_b^*)_x = \sigma\epsilon\,(T_{a,x}^4 - T_e^4)\,dS_a \tag{B19}$$

The heat lost by radiation from the externally finned version of the armor element when operating at surface temperature $T_{a,x}$ is, by definition, $(dQ)_x$. In steady state, when the heat lost by radiation is equal to the heat received by convection-and-conduction, $(dQ)_x$ has the value given by equation (B16).

Substituting equation (B16) for the left member of (B18), and using equation (B19) in the right member of (B18), the resulting equation is

$$U\,(T_{g,x} - T_{a,x})\,dS_a = \frac{(dQ)_x}{(dQ_b^*)_x}\left[\sigma\epsilon\,(T_{a,x}^4 - T_e^4)\,dS_a\right]$$

Cancelling the common term dS_a and dividing both sides of the equation by U,

$$T_{g,x} - T_{a,x} = \sigma\epsilon\left[\frac{(dQ)_x/(dQ_b^*)_x}{U}\right](T_{a,x}^4 - T_e^4) \qquad \text{(B20)}$$

Re-arranging (B20) so as to bring all terms involving $T_{a,x}$ to the left side of the equation,

$$T_{a,x} + \sigma\epsilon\left[\frac{(dQ)_x/(dQ_b^*)_x}{U}\right]T_{a,x}^4 = T_{g,x} + \sigma\epsilon\left[\frac{(dQ)_x/(dQ_b^*)_x}{U}\right]T_e^4 \qquad \text{(B21)}$$

Equation (B21) is the general form of the expression for the local armor temperature in terms of $(dQ)_x/(dQ_b^*)_x$ and other entering variables. Equation (30) of the Calculation Procedure is the same as equation (B21). Although in equation (30) both dQ and dQ_b^* change with x, the subscript x has been omitted from the ratio $(dQ)/(dQ_b^*)$. This has been done both to simplify the notation and to emphasize that for the class of radiators studied, the ratio $(dQ)/(dQ_b^*)$ is independent of x and has the same value at every axial station along the armor.

Derivation of the expression for $S_{a,x}$: The expression for the surface exposed by the armor to space in the axial distance from the radiator tube inlet to the station at x, equation (34) of the Calculation Procedure, is derived in this sub-section.

Differentiating equation (B20), treating ϵ and U as constants, transposing $dT_{a,x}$ to the right side of the equation, and dropping the subscript x with the understanding that only σ, ϵ, U and T_e are not x-dependent,

$$dT_g = dT_a + \frac{\sigma\epsilon}{U} \, d\left[\frac{(dQ)}{(dQ_b^*)}\left(T_a^4 - T_e^4\right)\right] \tag{B22}$$

From the heat balance for the gas,

$$-(\dot{m}c_p)dT_g = dQ \tag{B23}$$

Using (B18) and (B19) for dQ,

$$-(\dot{m}c_p)dT_g = \frac{(dQ)}{(dQ_b^*)}\left[\sigma\epsilon\,(T_a^4 - T_e^4)\right] dS_a \tag{B24}$$

Employing (B22) in (B24),

$$-(\dot{m}c_p)\left\{dT_a + \frac{\sigma\epsilon}{U} \, d\left[\frac{(dQ)}{(dQ_b^*)}\left(T_a^4 - T_e^4\right)\right]\right\}$$

$$= \frac{(dQ)}{(dQ_b^*)}\left[\sigma\epsilon\,(T_a^4 - T_e^4)\right] dS_a$$

Re-arranging this equation so that dS_a appears by itself on the left side of the equal sign, the expression for dS_a is

$$\left.\begin{aligned} dS_a = &- \frac{\dot{m}c_p}{\sigma\epsilon} \frac{dT_a}{\left[\frac{(dQ)}{(dQ_b^*)} (T_a^4 - T_e^4)\right]} \\ &- \frac{\dot{m}c_p}{U} \frac{d\left[\frac{(dQ)}{(dQ_b^*)} (T_a^4 - T_e^4)\right]}{\left[\frac{(dQ)}{(dQ_b^*)} (T_a^4 - T_e^4)\right]} \end{aligned}\right\} \quad (B25)$$

Integrating dS_a axially from the radiator tube entrance plane to station x,

$$\left.\begin{aligned} S_{a,x} = &- \frac{\dot{m}c_p}{\sigma\epsilon} \int_{T_{a,en}}^{T_{a,x}} \frac{dT_a}{\left[\frac{(dQ)}{(dQ_b^*)} (T_a^4 - T_e^4)\right]} \\ &- \frac{\dot{m}c_p}{U} \ln\left\{ \frac{\left[\frac{(dQ)}{(dQ_b^*)}\right]_x (T_{a,x}^4 - T_e^4)}{\left[\frac{(dQ)}{(dQ_b^*)}\right]_{en} (T_{a,en}^4 - T_e^4)} \right\} \end{aligned}\right\} \quad (B26)$$

Equation (B26) is the general form for $S_{a,x}$ in terms of the variable $(dQ)/(dQ_b^*)$. In the derivation of equation (B26), no restriction has been placed on the manner in which $(dQ)/(dQ_b^*)$ may vary; hence it may vary in any desired manner, consistent with the overall thermal and pressure performance required of the radiator. One possible

prescription is that $(dQ)/(dQ_b^*)$ shall have the same value at all axial stations of the radiator; another, less direct, but definitive prescription is that $(dQ)/(dQ_b^*)$ shall vary so as to keep the thickness of the external fins constant along the entire length of the radiator tubes. Other specifications on $(dQ)/(dQ_b^*)$ are also possible; each specification leads to characteristic properties of the external fins.

For ease of calculation in the present study, $(dQ)/(dQ_b^*)$ was specified to have a single constant value for the entire radiator. Under this specification, equation (B26) is reduced to the simple form

$$\left.\begin{aligned} S_{a,x} = &- \frac{1}{\sigma\epsilon} \frac{\dot{m}c_p}{(dQ)/(dQ_b^*)} \int_{T_{a,en}}^{T_{a,x}} \frac{dT_a}{T_a^4 - T_e^4} \\ &- \frac{\dot{m}c_p}{U} \ln\left(\frac{T_{a,x}^4 - T_e^4}{T_{a,en}^4 - T_e^4}\right) \end{aligned}\right\} \qquad \text{(B27)}$$

Performing the indicated integration, re-arranging the logarithmic expression so as to obtain a positive algebraic sign, and writing $\dot{m}c_p/U$ in the equivalent form

$$\frac{\dot{m}c_p}{U} \equiv \frac{\dot{m}c_p / \left[(dQ)/(dQ_b^*)\right]}{U / \left[(dQ)/(dQ_b^*)\right]} \quad ,$$

equation (B27) becomes

$$S_{a,x} = \frac{\dot{m}c_p}{(dQ)/(dQ_b^*)} \frac{1}{\sigma\epsilon} \frac{1}{4T_e^3} \left[\ln\left(\frac{T_{a,x} + T_e}{T_{a,en} + T_e} \frac{T_{a,en} - T_e}{T_{a,x} - T_e} \right) + \right.$$

$$\left. + \; 2\tan^{-1}\left(\frac{T_{a,x}}{T_e}\right) - 2\tan^{-1}\left(\frac{T_{a,en}}{T_e}\right) \right] \; + \qquad \text{(B28)}$$

$$+ \frac{\dot{m}c_p / \left[(dQ)/(dQ_b^*)\right]}{U \; / \left[(dQ)/(dQ_b^*)\right]} \ln\left(\frac{T_{a,en}^4 - T_e^4}{T_{a,x}^4 - T_e^4} \right)$$

Equation (B28) is the same as equation (34) of the Calculation Procedure.

Comments: In the foregoing discussion, the heat radiated by an element of armor and its external fins, dQ, has been expressed in terms of the heat radiated by an element of bare armor surface, dQ_b^*, as given by equation (B19). It would have been possible to omit all references to bare armor radiators and to postulate that the heat release of the armor and its external fins, dQ, is expressible in the form

$$dQ = \varphi(x)\left[\sigma\epsilon \; (T_{a,x}^4 - T_e^4) dS_a \right]$$

with $\varphi(x)$ a function of x whose form requires determination and is governed by input specifications. It is instructive, however,

to retain the concept of a reference bare armor radiator, because thereby the close relationships that exist between bare and finned armor radiators are kept in view. For example, the data of References 2 and 3 show that the heat release of a finned armor radiator is expressible conveniently and naturally as a multiple of the heat release of a bare armor radiator.

A relationship between externally finned and externally bare armor radiators of interest in the present study is as follows: The class of externally finned radiators that operates with the same value of $(dQ)/(dQ_b^*)$ over the entire armor surface has fluid and armor temperature fields, and surface area of armor, that are identical with those of bare armor radiators which satisfy the conditions

$$\left.\begin{aligned}
T_{e,b} &= T_e \text{ of finned armor radiator} \\
\epsilon_b &= \epsilon \quad " \\
(T_{g,en})_b &= T_{g,en} \quad " \\
(T_{g,ex})_b &= T_{g,ex} \quad " \\
(dQ)/(dQ_b^*) &= \text{constant} \\
(\dot{m}c_p)_b &= \frac{\dot{m}c_p}{(dQ)/(dQ_b^*)} \quad " \\
U_b &= \frac{U}{(dQ)/(dQ_b^*)} \quad " \\
(dS_a)_b &= dS_a \quad "
\end{aligned}\right\} \qquad \text{(B29)}$$

The condition $(dS_a)_b = dS_a$ implies that equal increments of armor surface are to be considered when comparing the axial progress of T_g, T_a, and dQ in the externally bare and externally finned armor radiators.

The identity of gas and armor temperature fields, and of armor surface areas, of bare and finned armor radiators that satisfy (B29) is readily established by use of equations (B21), (B24) and the condition $(dS_a)_b = dS_a$. The relationship between bare and finned armor radiators that satisfy (B29) can be used as a basis for a calculation procedure which produces numerical results identical with those reported herein.

REFERENCES

1. Glassman, A. J. : Summary of Brayton Cycle Analytical Studies for Space-Power System Applications. NASA TN D-2487, Sept. 1964.

2. Sparrow, E. M. and Eckert, E. R. G. : Radiant Interaction Between Fin and Base Surfaces. Trans. ASME, Jnl of Heat Transfer, Feb. 1962.

3. Sparrow, E. M. ; Miller, G. B. ; and Jonsson, V. K. : Radiating Effectiveness of Annular-Finned Space Radiators, Including Mutual Irradiation Between Radiator Elements. Jnl Aerosp. Sc., Nov. 1962.

4. Loeffler, I. J. ; Lieblein, S. ; and Clough, N. : Meteoroid Protection for Space Radiators. NASA Paper 2543-62, prepared for ARS Space Power Systems Conf. at Santa Monica, Calif. , Sept. 25-28, 1962.

5. Sparrow, E. M. ; Jonsson, V. K. ; and Minkowycz, W. J. : Heat Transfer from Fin-Tube Radiators, Including Longitudinal Heat Conduction and Radiant Interchange Between Longitudinally Nonisothermal Finite Surfaces. NASA TN D-2077, Dec. 1963.

6. Humble, L. V. ; Lowdermilk, W. H. ; and Desmon, L. G. : Measurements of Average Heat-Transfer and Friction Coefficients for Subsonic Flow of Air in Smooth Tubes at High Surface and Fluid Temperatures. NACA Report 1020, 1951.

7. McAdams, W. H. : Heat Transmission. McGraw-Hill Book Co., New York, 1954, p. 268.

8. Diedrich, J. H. and Lieblein, S. : Materials Problems Associated With the Design of Radiators for Space Powerplants. Paper prepared for ARS Space Power Systems Conference, Santa Monica, Calif., Sept. 25-28, 1962.

9. DeLorenzo, B. ; and Anderson, E. D. : Heat Transfer and Pressure Drop of Liquids in Double-Pipe Fin-Tube Exchangers. Trans. ASME, Nov. 1945.

10. Kays, W. M. ; and London, A. L. : Compact Heat Exchangers, McGraw-Hill Book Co., Inc., New York, 1958, fig. 84 and Table 20.

11. Svehla, R. A. : Estimated Viscosities and Thermal Conductivities of Gases at High Temperatures. NASA TR R-132, 1962.

12. Saule, A. V. ; Krebs, R. P. ; and Auer, B. M. : Design Analysis and General Characteristics of Flat-Plate Central-Fin-Tube Sensible Heat Radiators. NASA TN D-2839, June, 1965.

13. Jakob, M. : Heat Transfer, Vol. I, John Wiley & Sons, Inc., New York, 1949, p. 132.

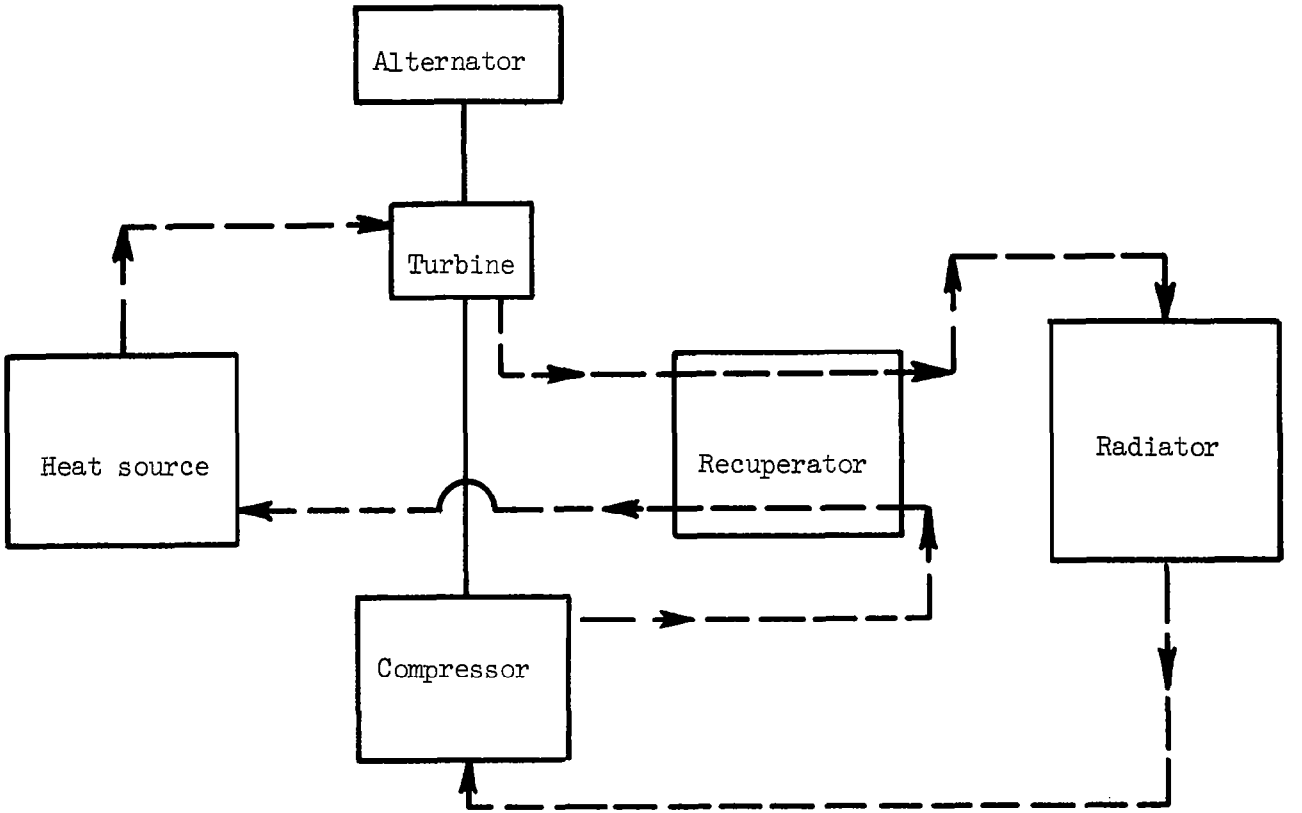

Figure 1. - Brayton cycle with gaseous working fluid in radiator.

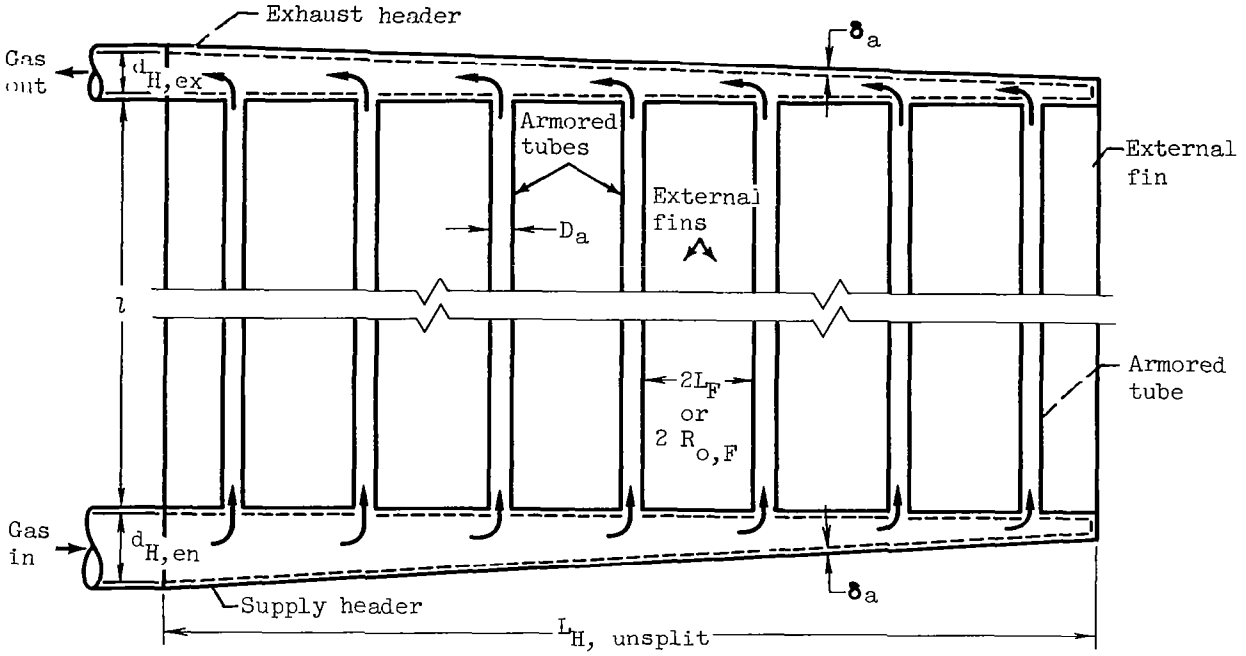

(a) Radiator with unsplit headers (schematic).

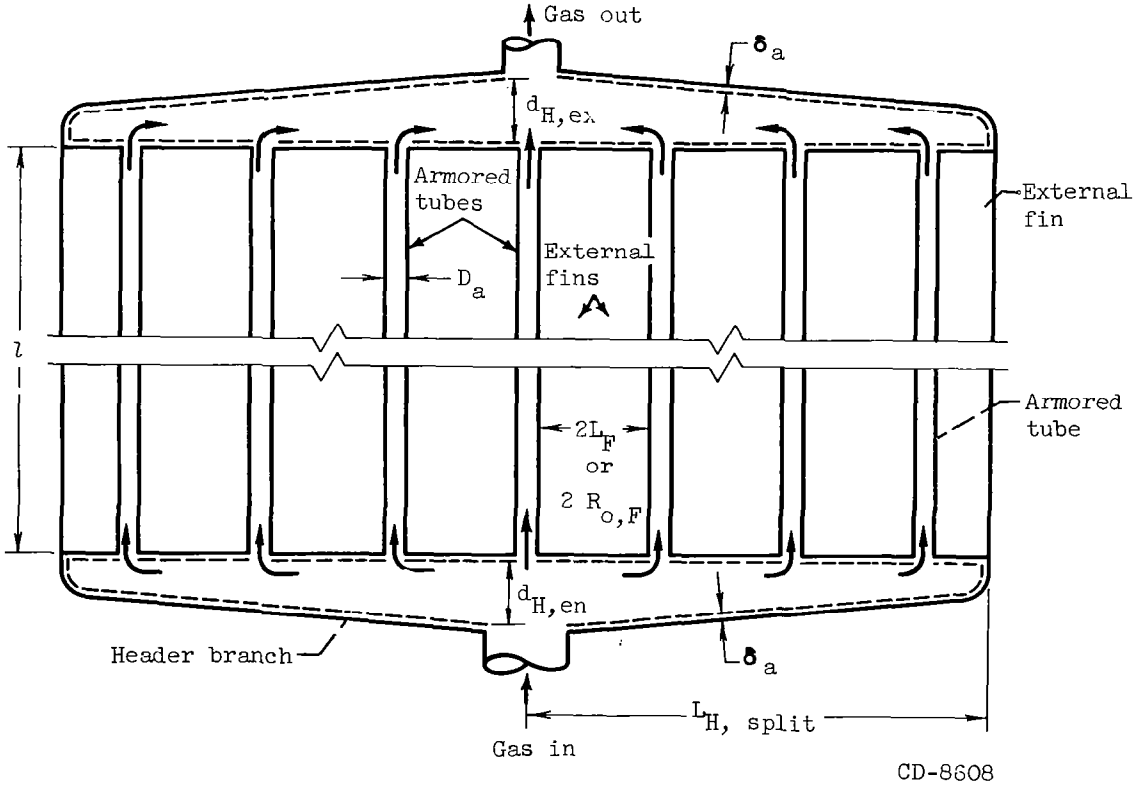

(b) Radiator with once-split headers (schematic).

Figure 2. - Radiator and header arrangements.

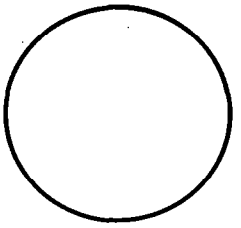

(a) Internally unfinned tube.

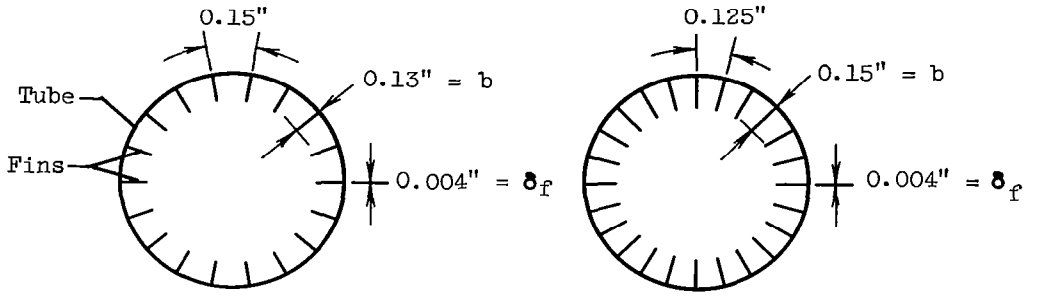

(b) Short radial fins.

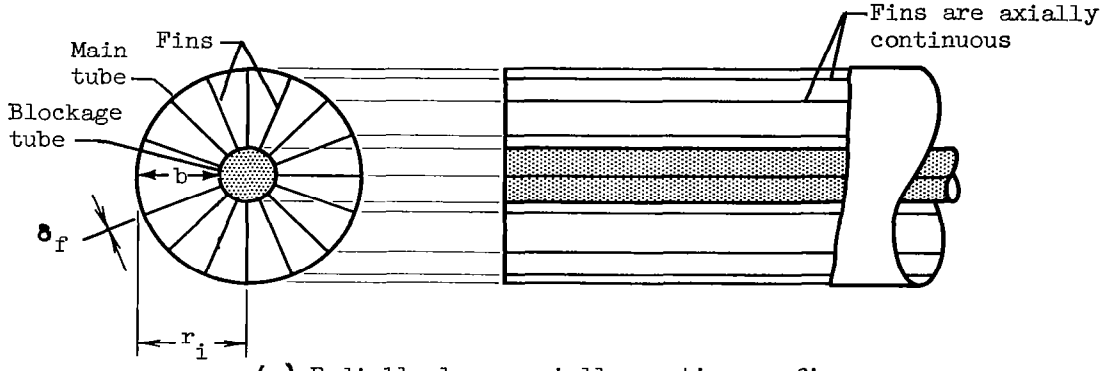

(c) Radially long, axially continuous fins.

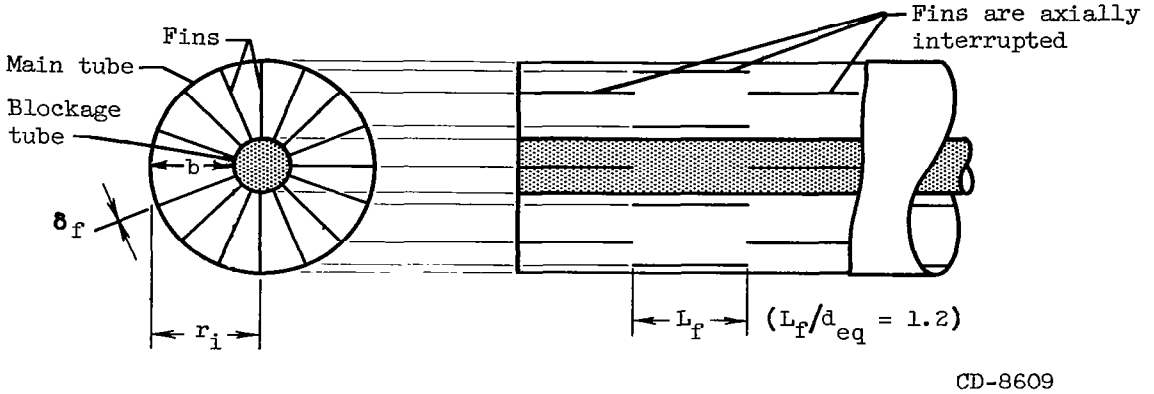

(d) Radially long, axially interrupted fins.

Figure 3. - Principal internal geometries studied.

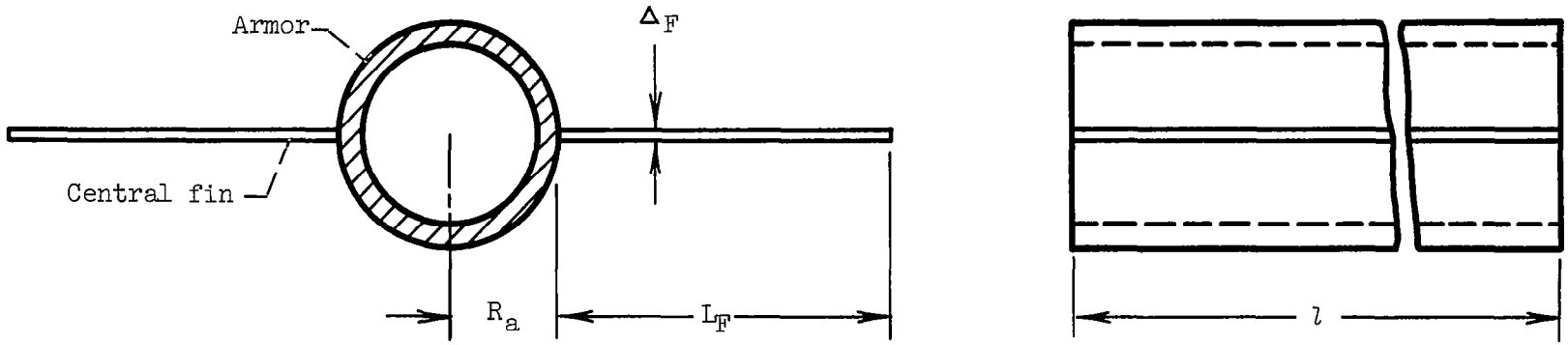

CD-8610

Figure 4. - Radiator tube with central external fins.

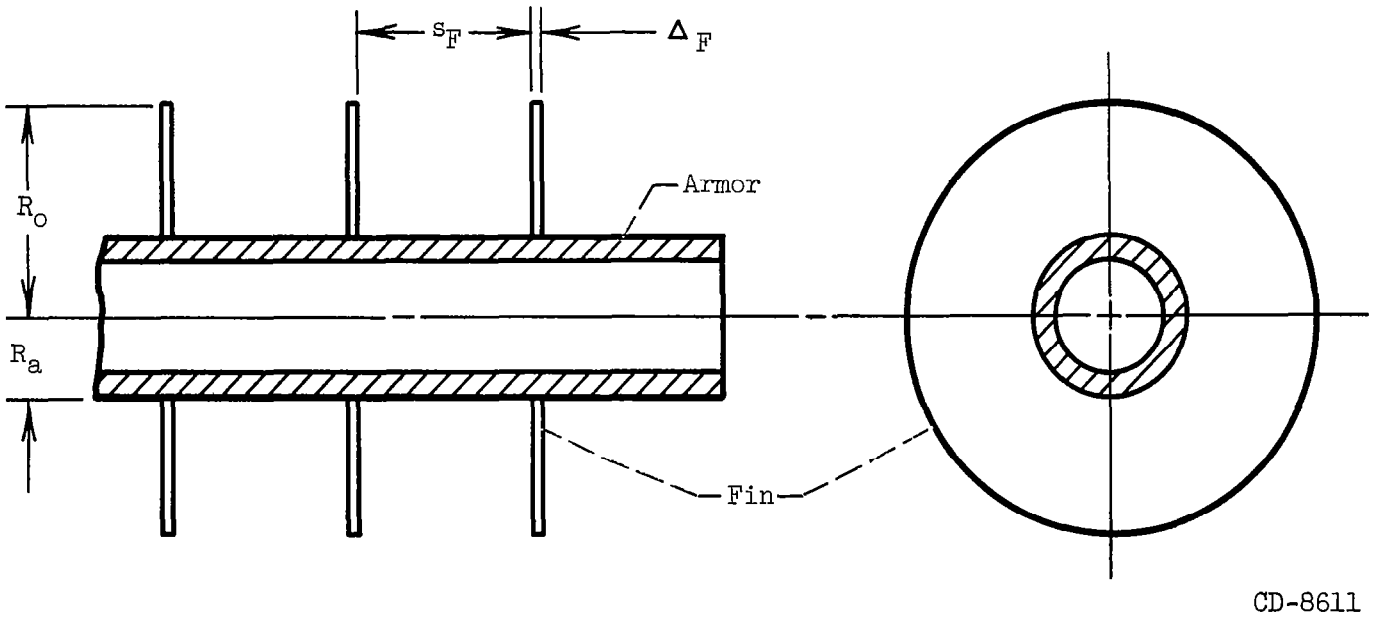

Figure 5. - Radiator tube with circumferential external fins.

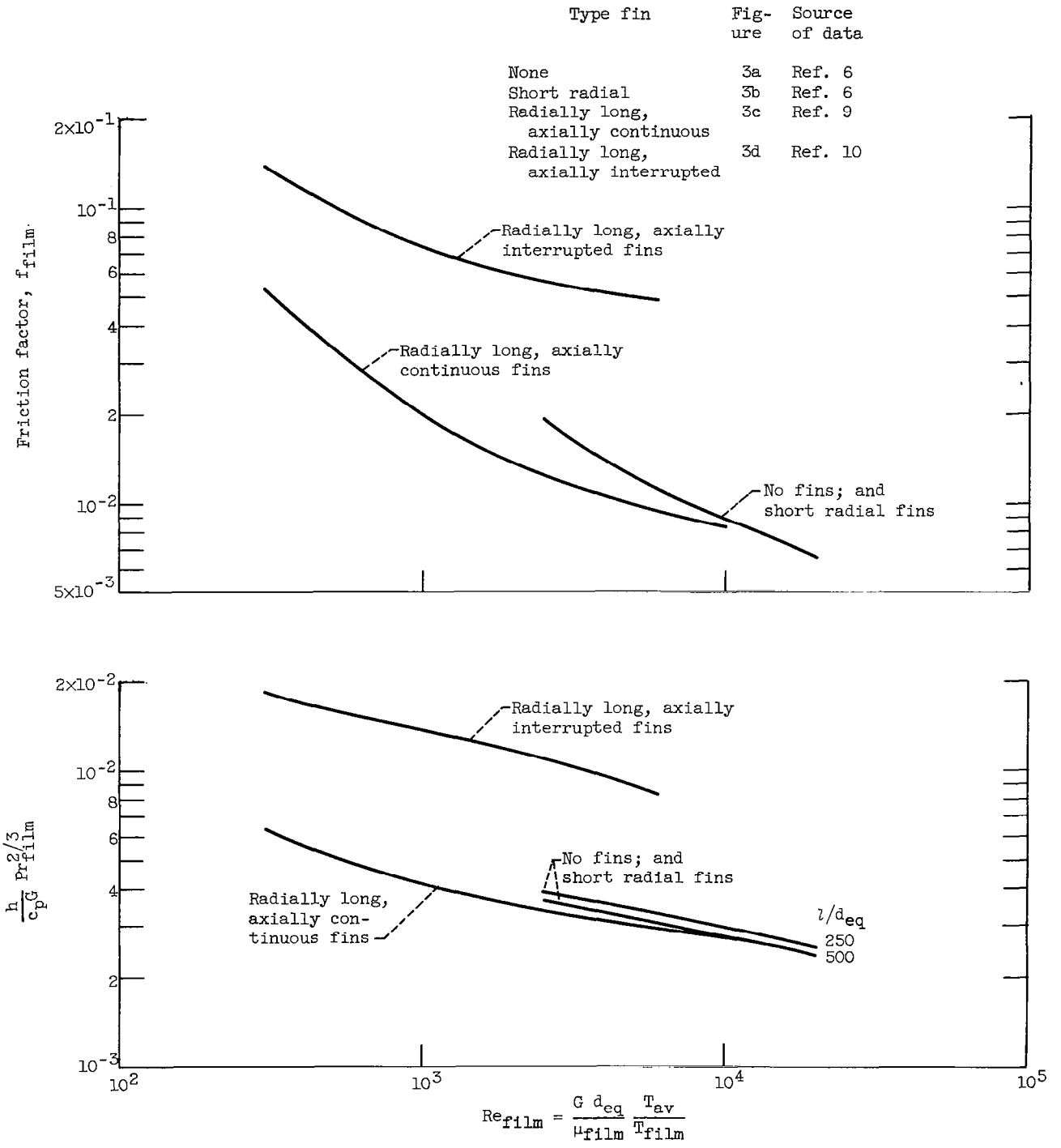

Figure 6. - Heat transfer coefficients and friction factors.

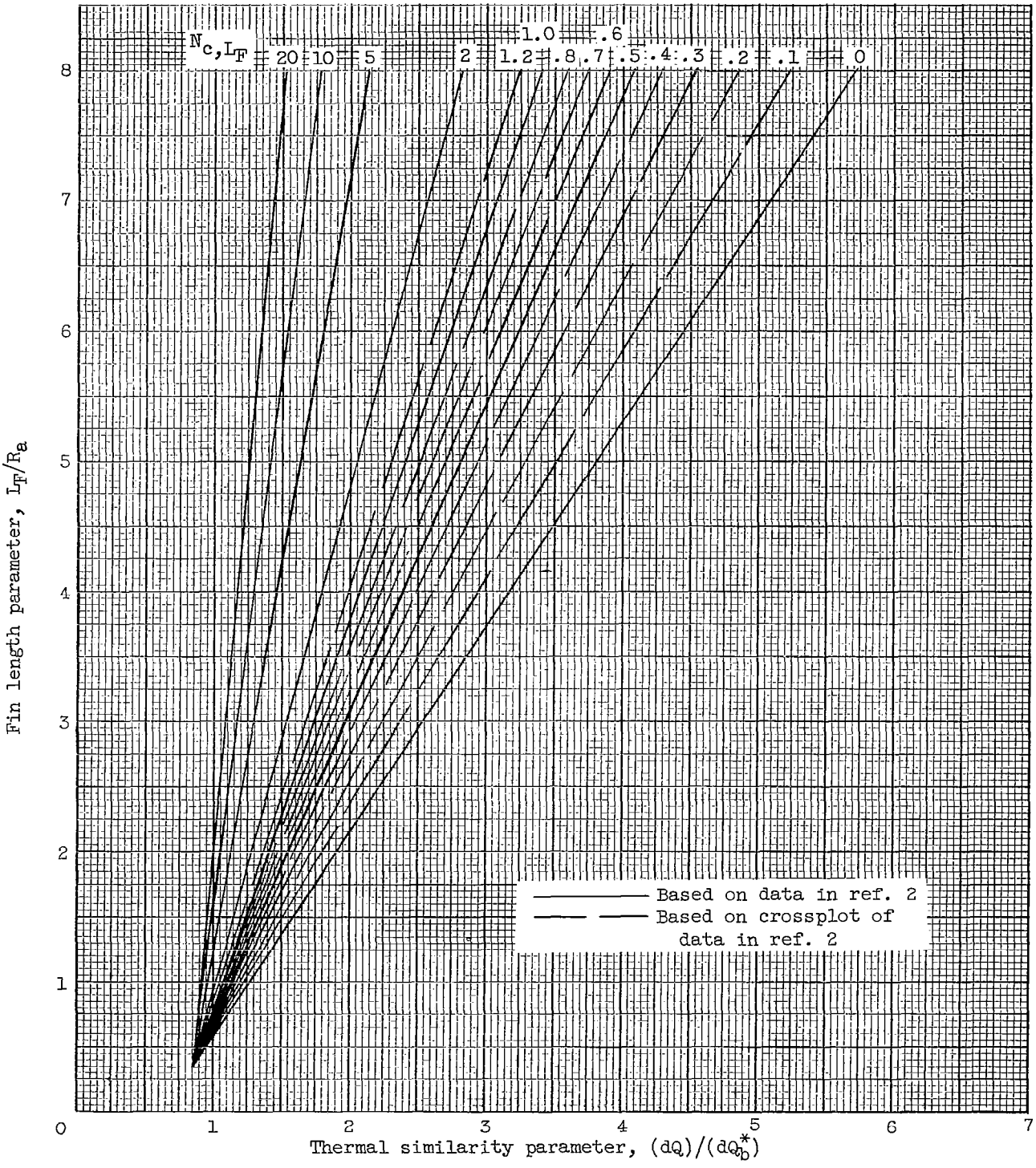

Figure 7. - Fin length parameter versus $(dQ)/(dQ_b^*)$ and N_{c,L_F} for central external fins.

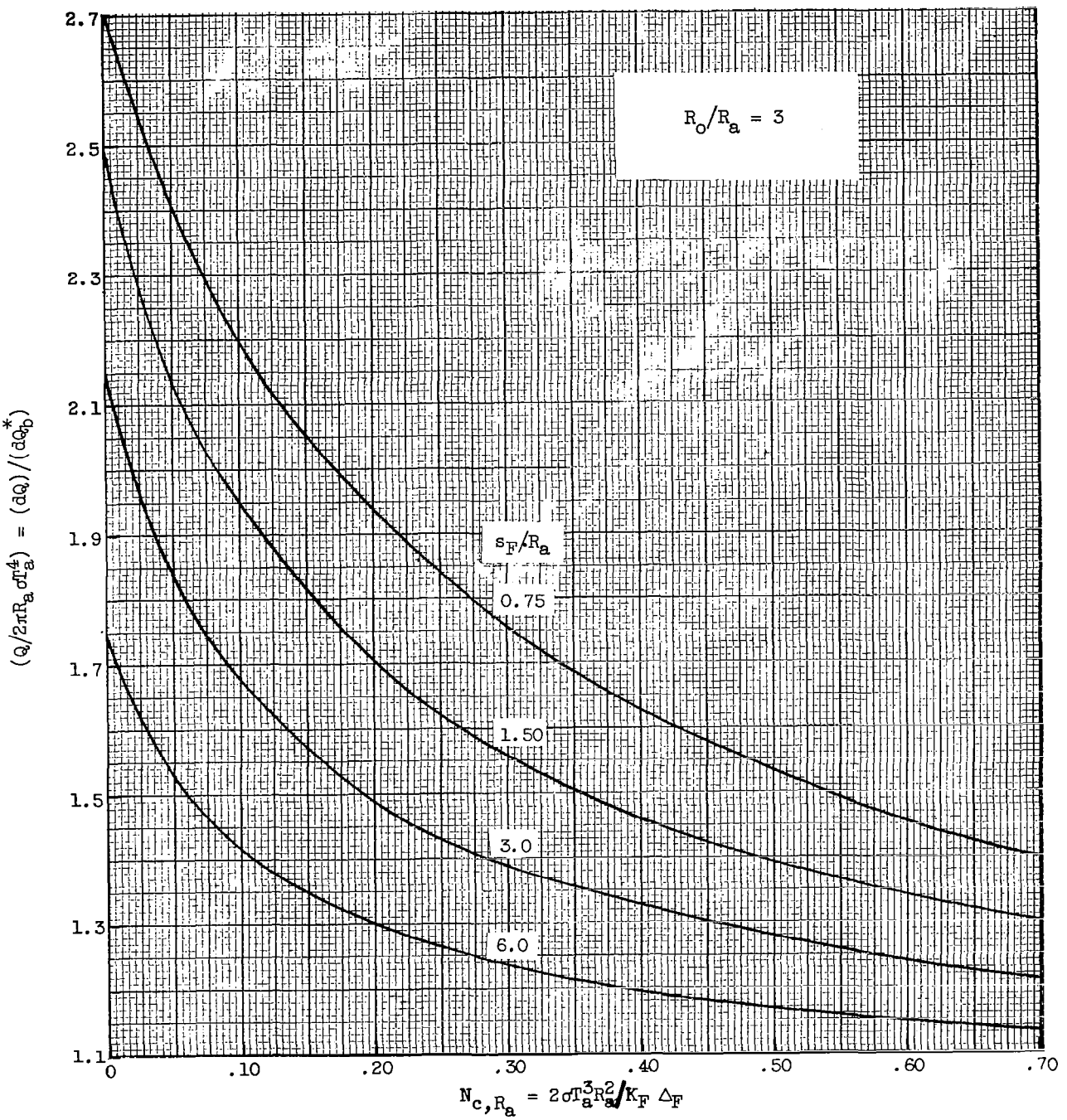

Figure 8. - Illustrative theoretical performance curves for radiators with circumferential external fins (ref. 3).

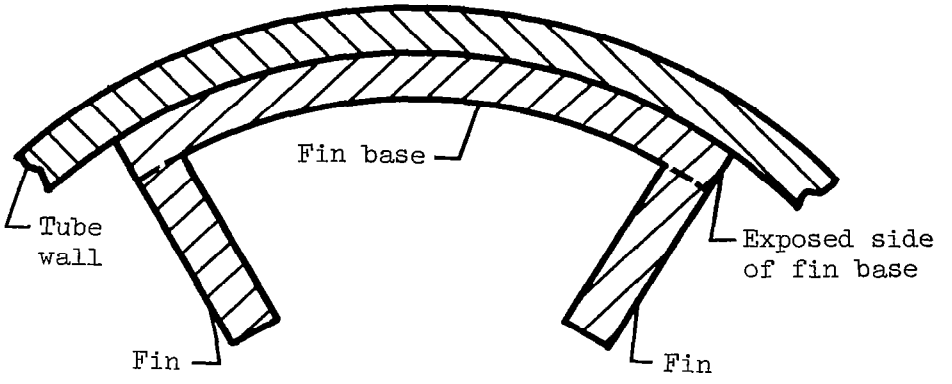

(a) Finned tube detail.

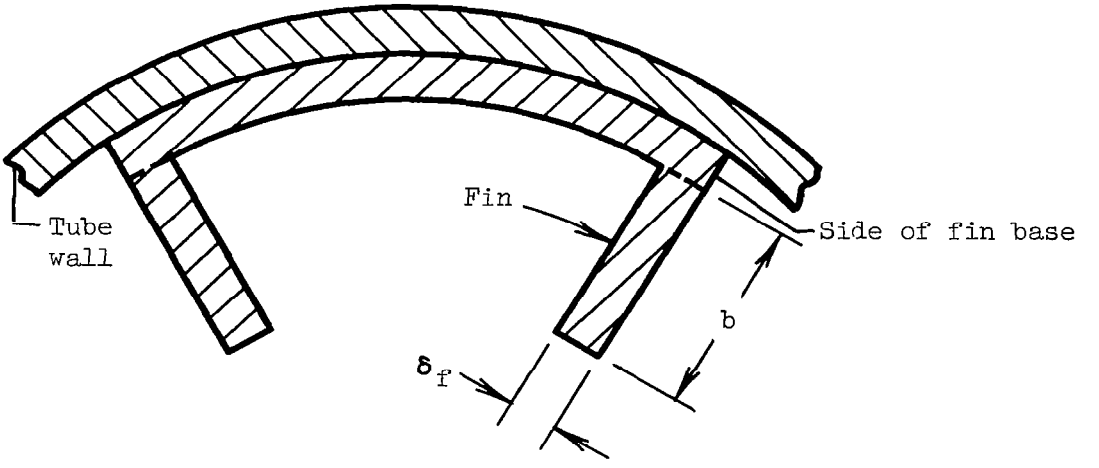

CD-8612

(b) Fin symbols.

Figure 9. - Geometric details and nomenclature of internally finned tubes.

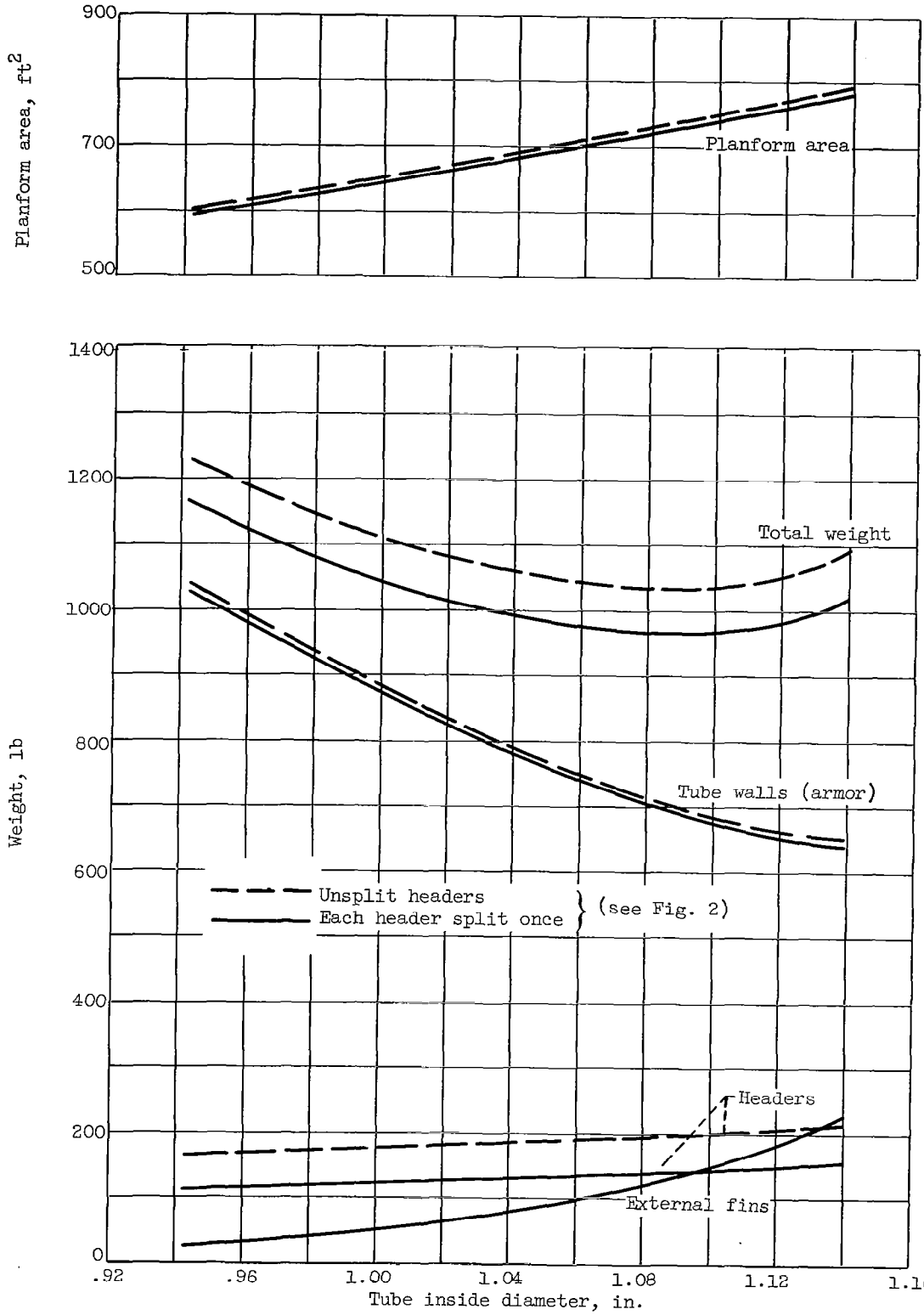

Figure 10. - Effect of tube inside diameter in internally unfinned radiators; l_{tube} = 25 ft, central external fins, N_{c,L_F} = 1.0.

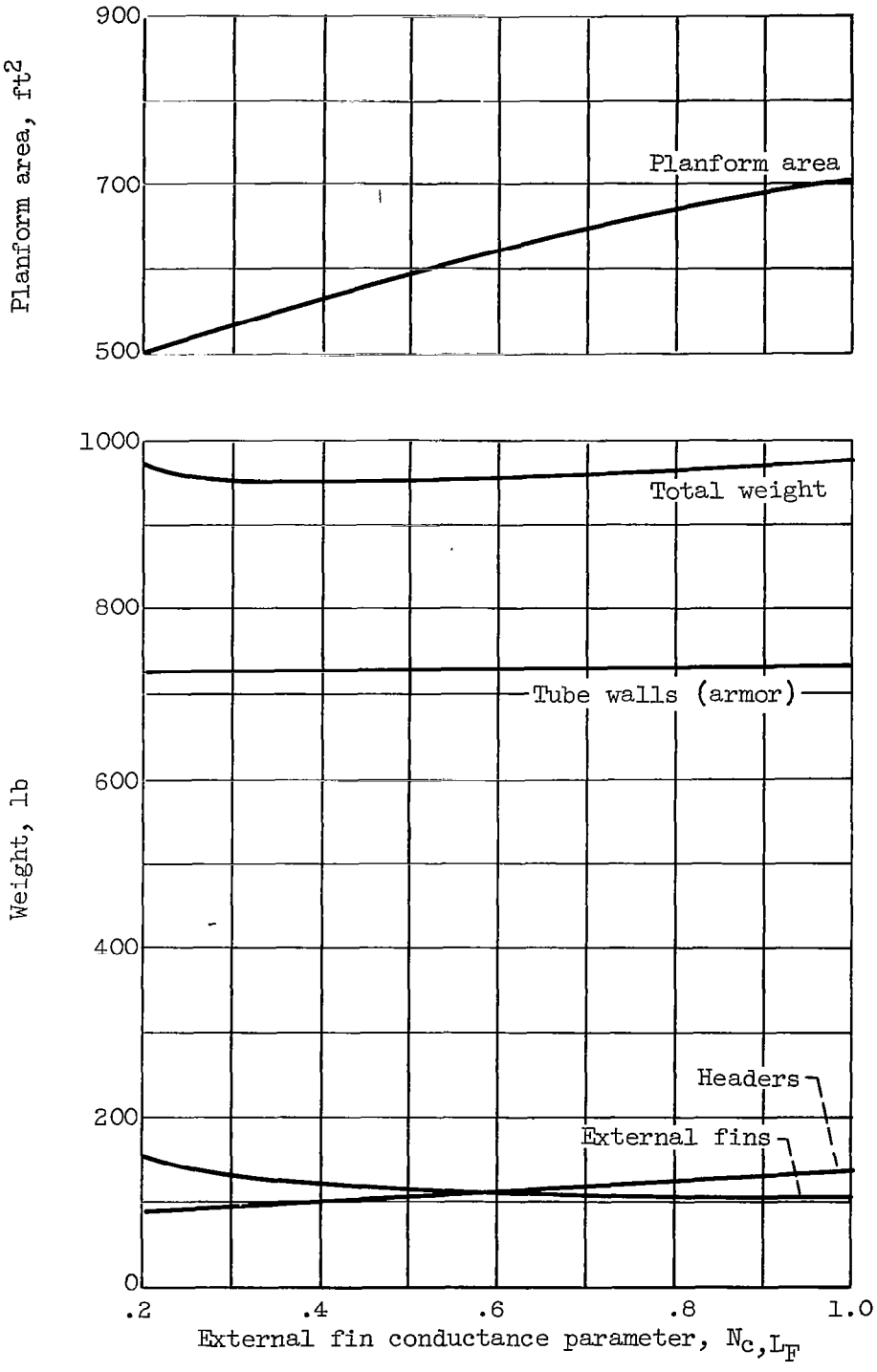

Figure 11. - Effect of N_{c,L_F} in internally unfinned radiators; l_{tube} = 25 ft, central external fins, d_i = 1.07 inch, headers split once.

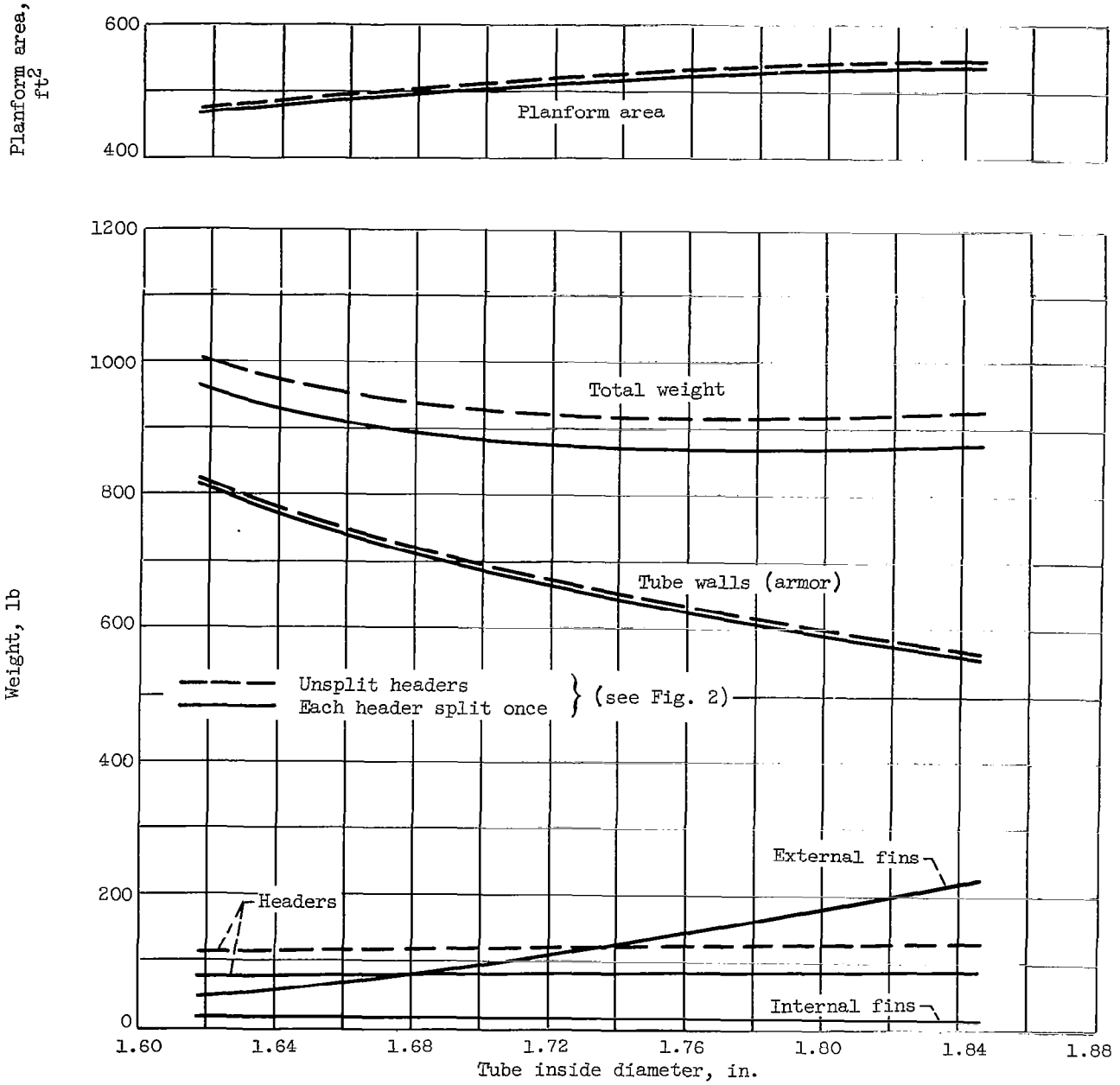

Figure 12a. - Effect of tube inside diameter in internally finned radiators; "short radial - I" internal fins (Fig. 3b), l_{tube} = 25 ft, central external fins, N_c, L_F = 1.0.

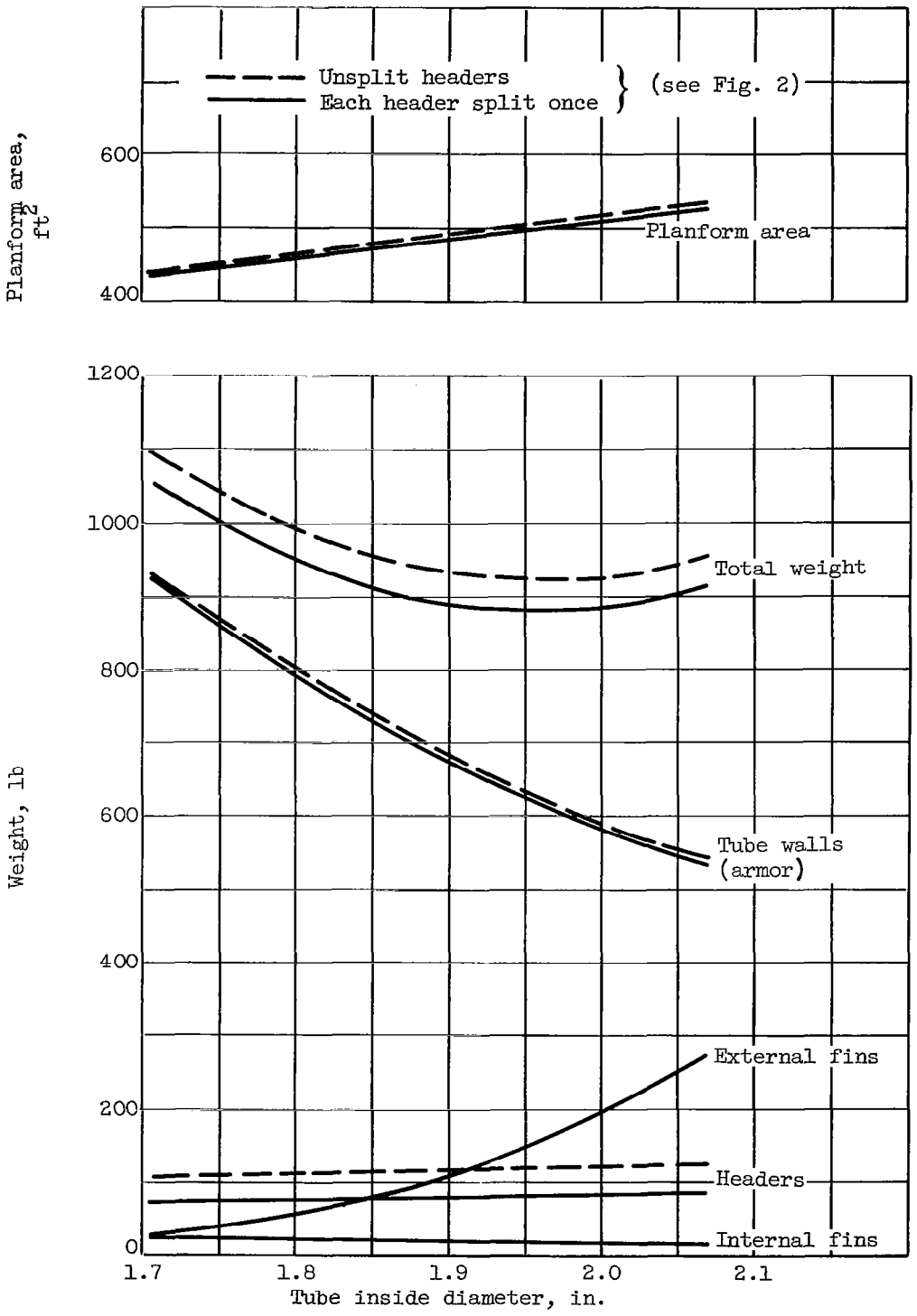

Figure 12b. - Effect of tube inside diameter in internally finned radiators; "short radial - II" internal fins (Fig. 3b), l_{tube} = 25 ft, central external fins, N_{c,L_F} = 1.0.

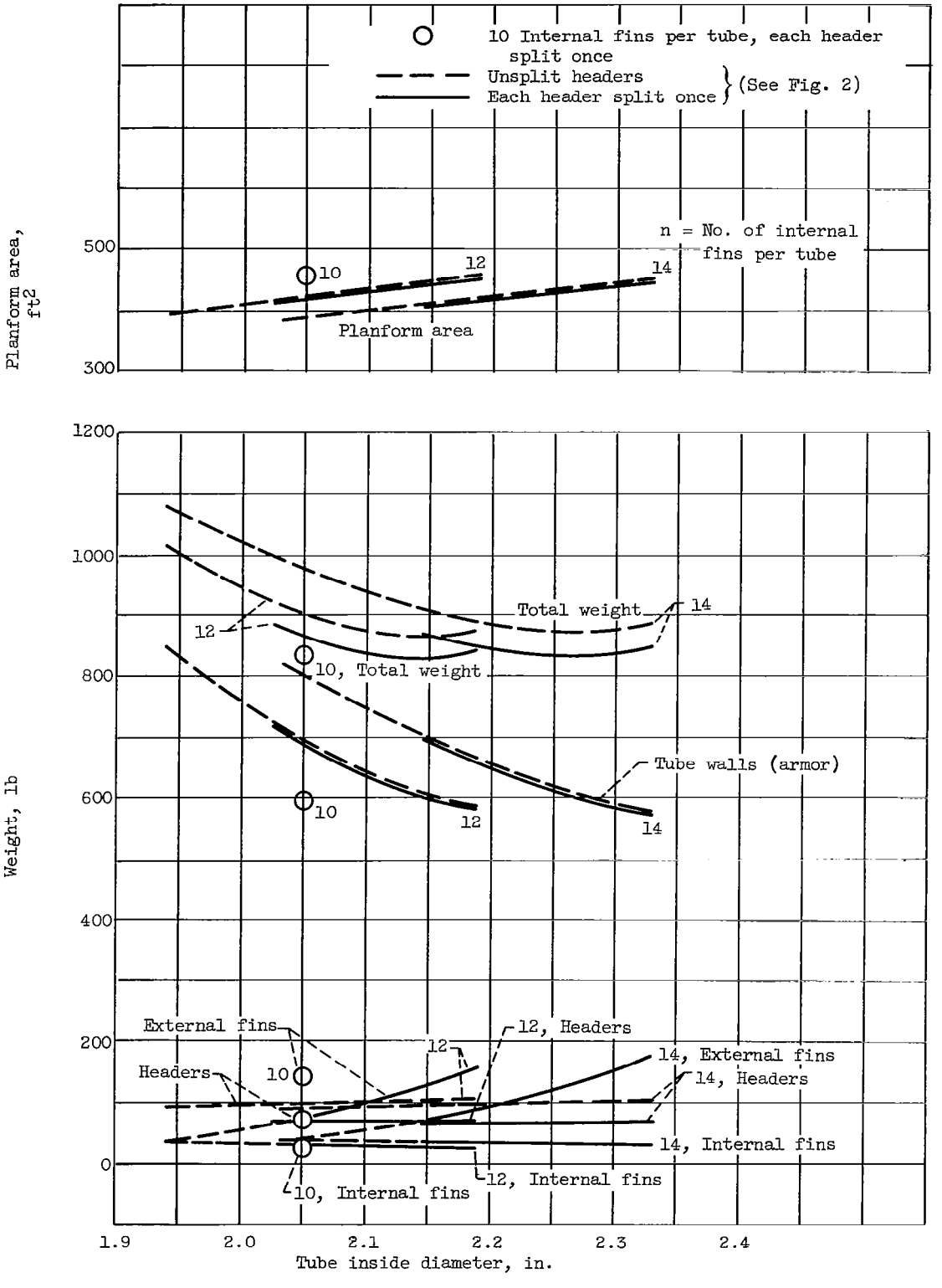

Figure 13. - Effect of tube inside diameter and of number of internal fins per tube; radially long, axially continuous internal fins (Fig. 3c), l_{tube} = 25 ft, central external fins, N_{c,L_F} = 1.0.

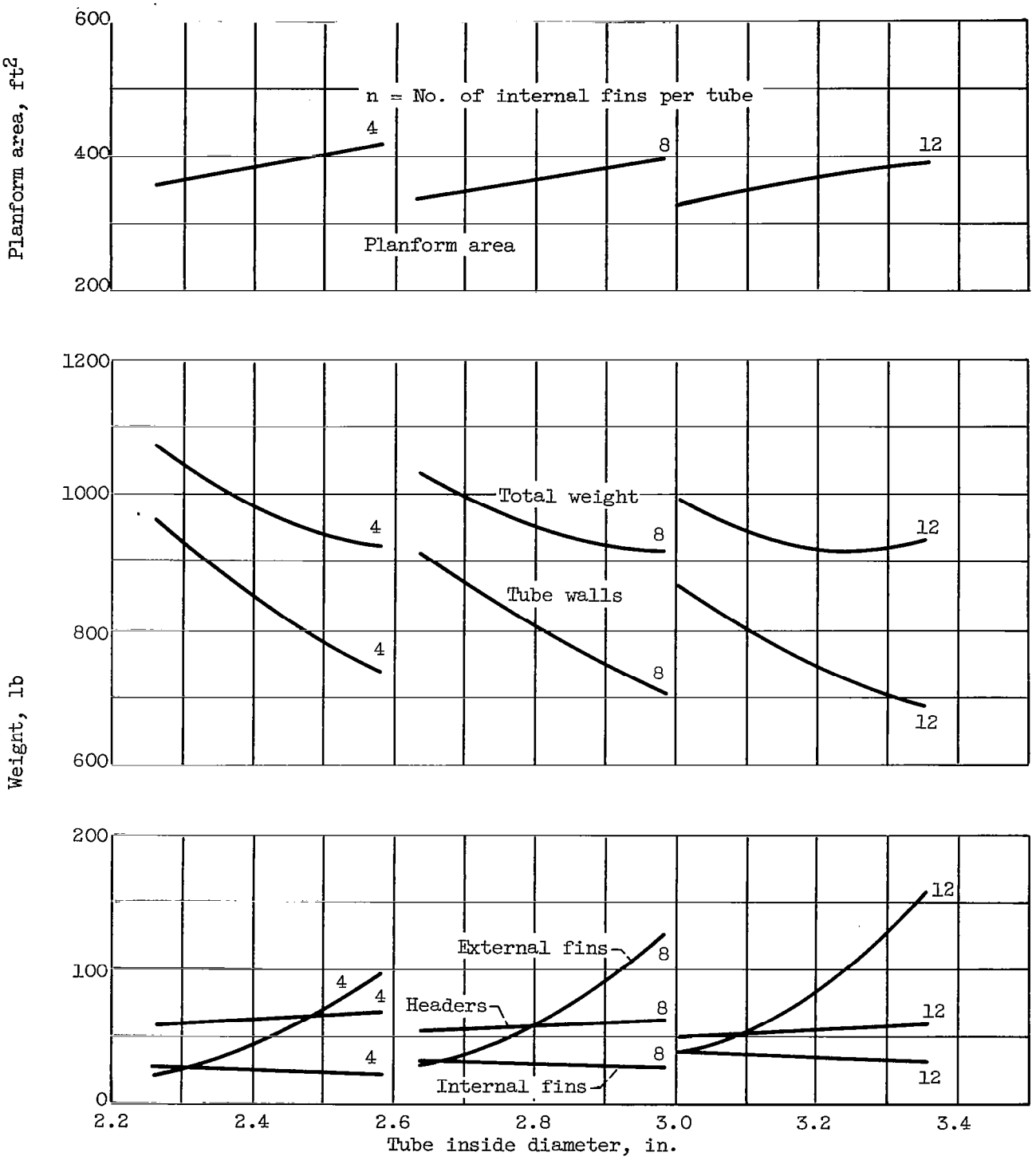

Figure 14. - Effect of tube inside diameter and of number of internal fins per tube; axially interrupted fins (Fig. 3d), l_{tube} = 25 ft, central external fins, N_{c,L_F} = 1.0, each header split once (see Fig. 2).

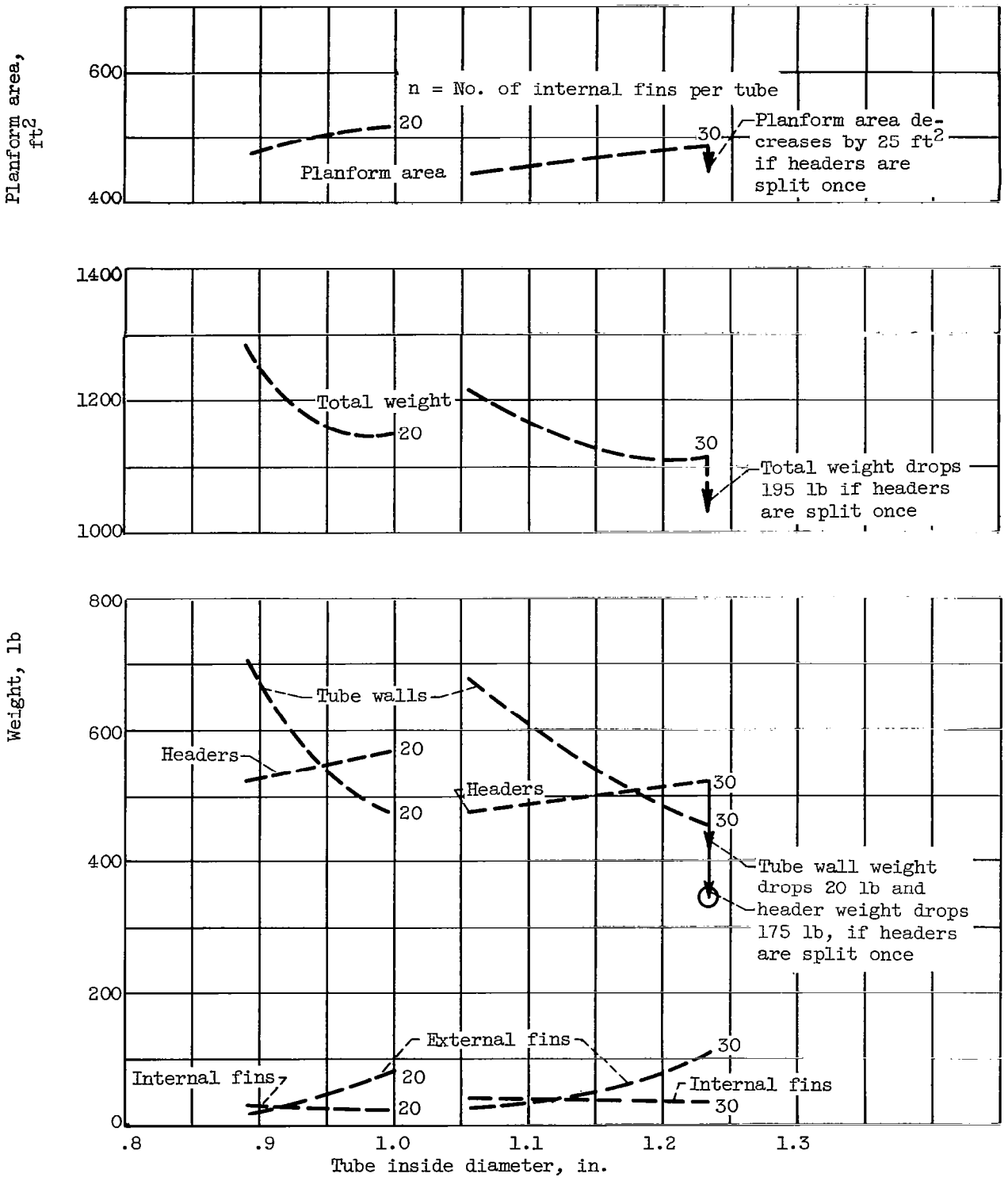

Figure 15. - Effect of tube inside diameter and of number of internal fins per tube; radially long, axially continuous internal fins (Fig. 3c), l_{tube} = 6 ft, central external fins, N_{c,L_F} = 1.0, headers unsplit (see Fig. 2).

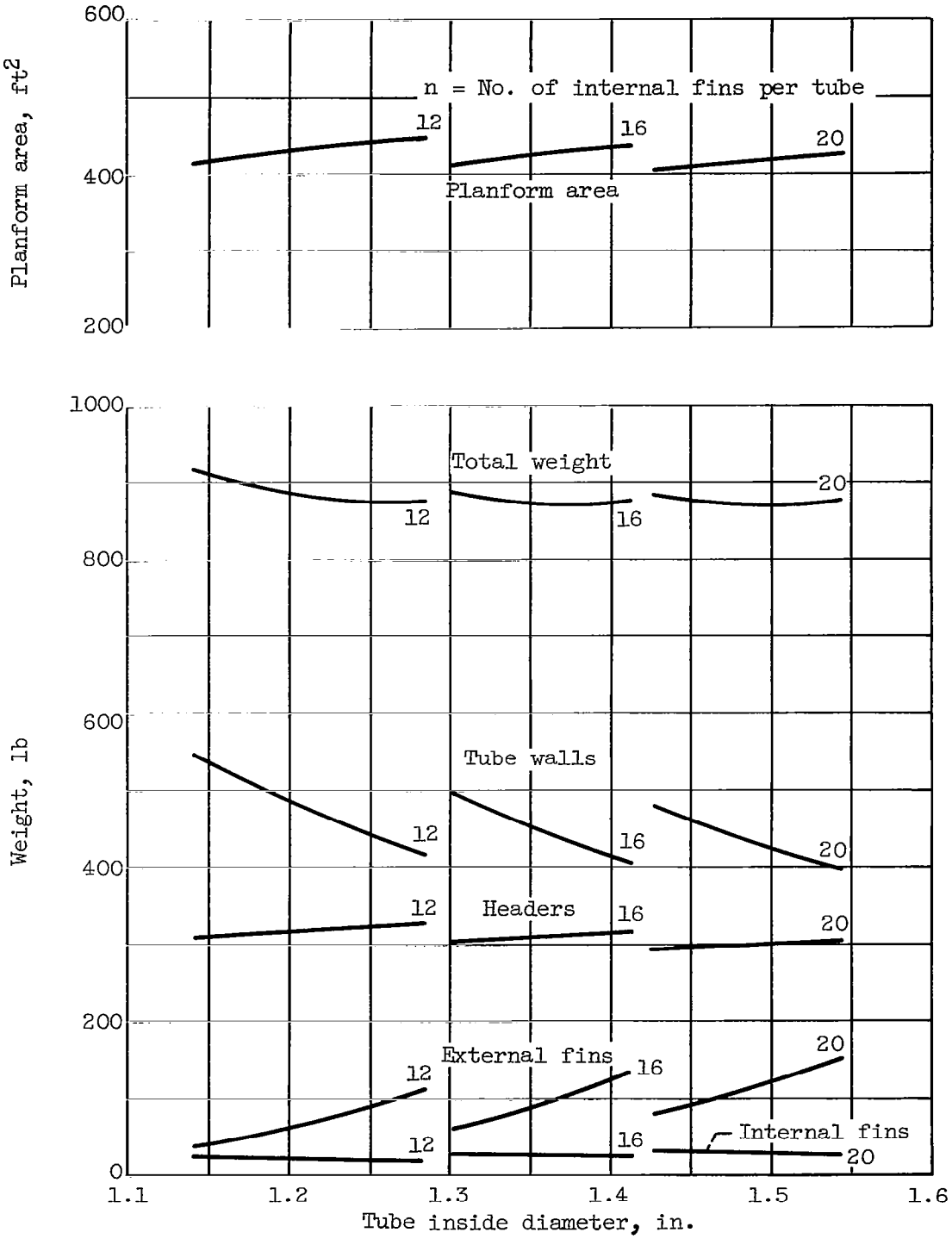

Figure 16. - Effect of tube inside diameter and of number of internal fins per tube; axially interrupted fins (Fig. 3d), l_{tube} = 6 ft, central external fins, N_c, L_F = 1.0, each header split once (see Fig. 2).

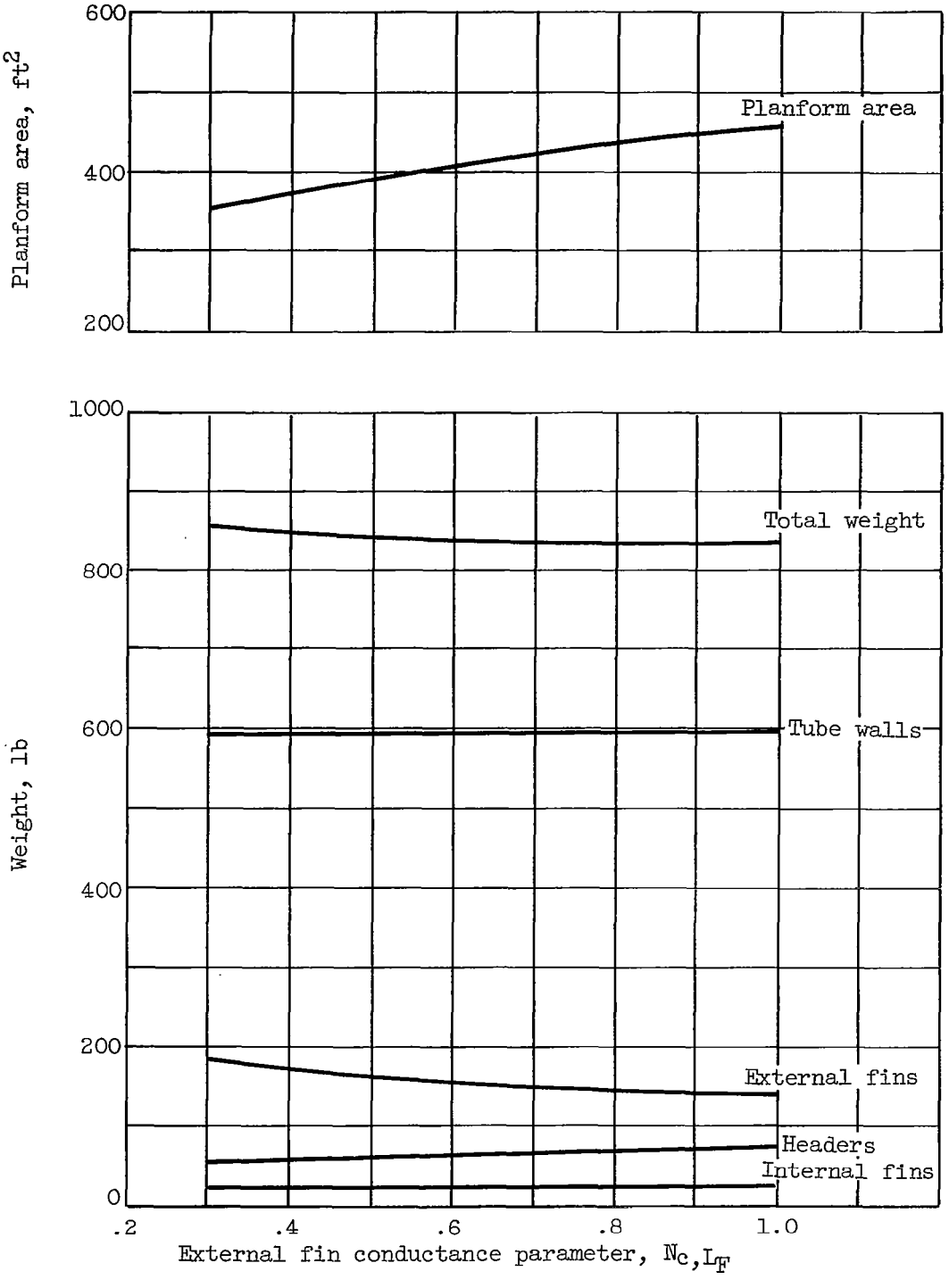

Figure 17. - Effect of external fin conductance parameter; radially long, axially continuous internal fins (Fig. 3c), l_{tube} = 25 ft, central external fins, tube inside diameter = 2.05 inch, 10 internal fins/tube, each header split once (see Fig. 2).

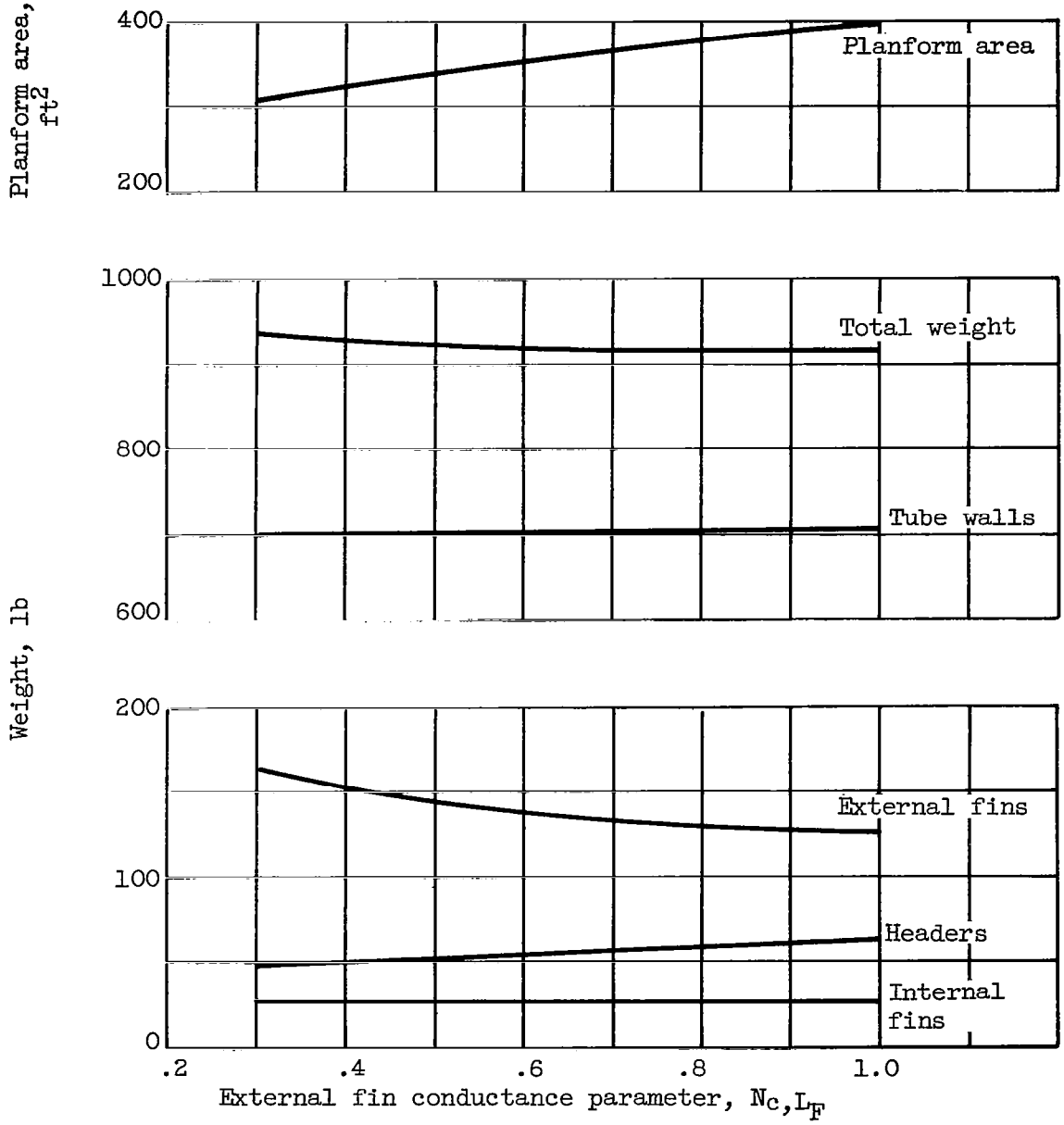

Figure 18. - Effect of external fin conductance parameter; axially interrupted internal fins (Fig. 3d), l_{tube} = 25 ft, central external fins, tube inside diameter = 2.98 inch, 8 internal fins/tube, each header split once (see Fig. 2).

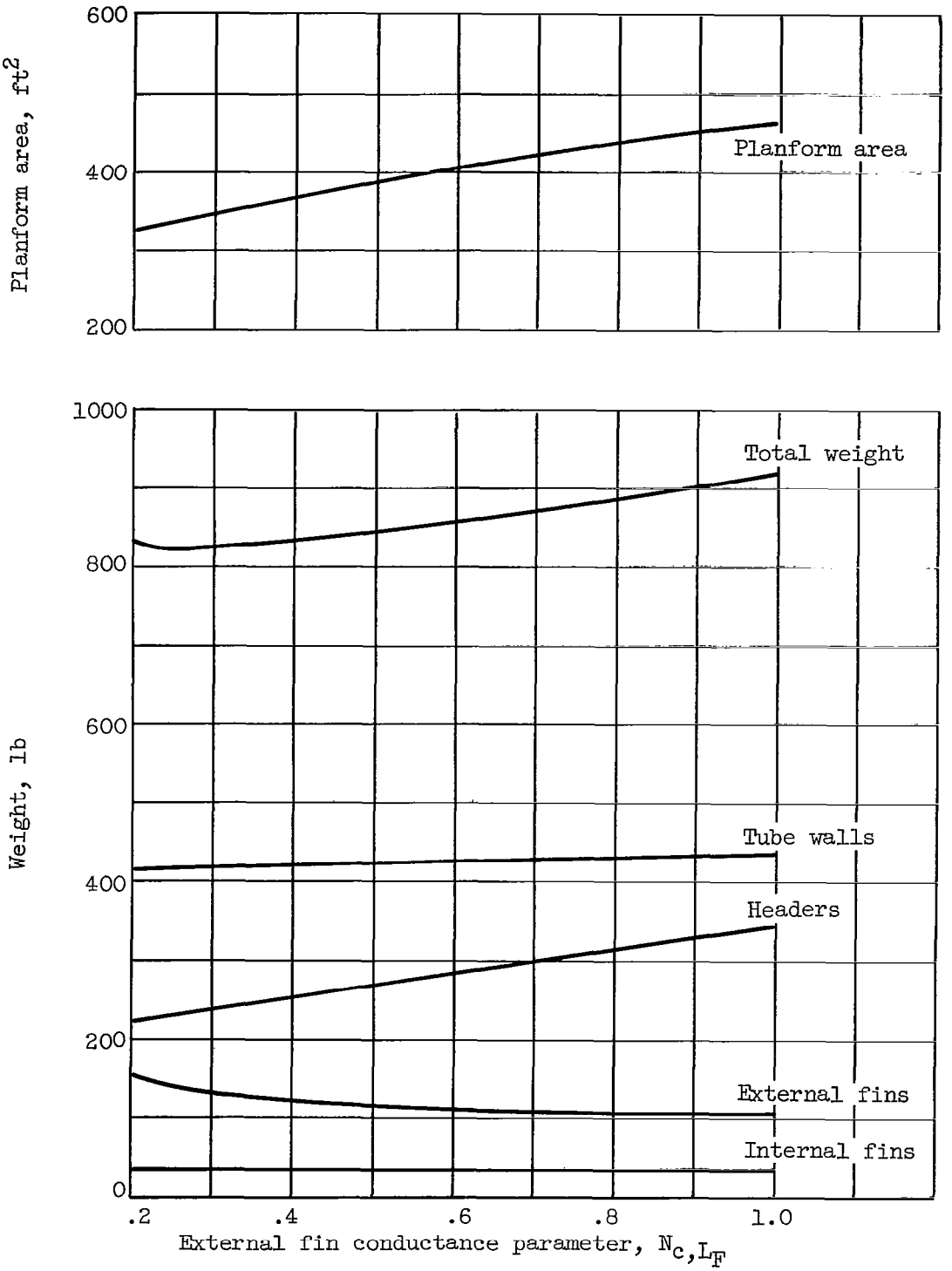

Figure 19. - Effect of external fin conductance parameter; radially long, axially continuous internal fins (Fig. 3d), l_{tube} = 6 ft, central external fins, tube inside diameter = 1.23 inch, 30 internal fins/tube, each header split once (see Fig. 2).

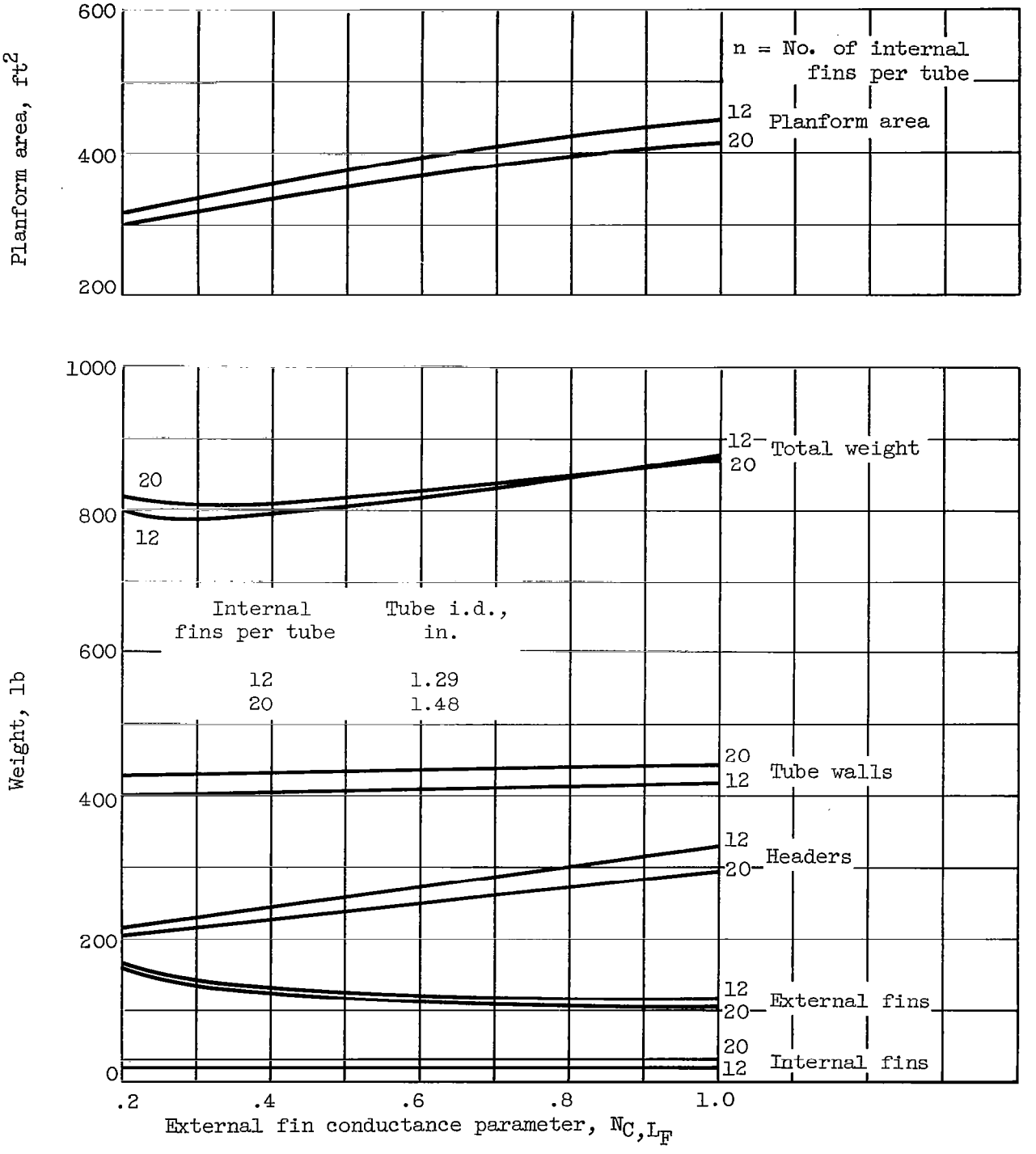

Figure 20. - Effect of N_{C,L_F} and of number of internal fins per tube; axially interrupted internal fins (Fig. 3d), l_{tube} = 6 ft, central external fins, each header split once (see Fig. 2).

Internal fins per tube	Type of internal fin	Tube length (ft)	Tube i.d. (inch)
0	None	25	1.07
12	Axially interrupted (Fig. 3d)	6	1.29

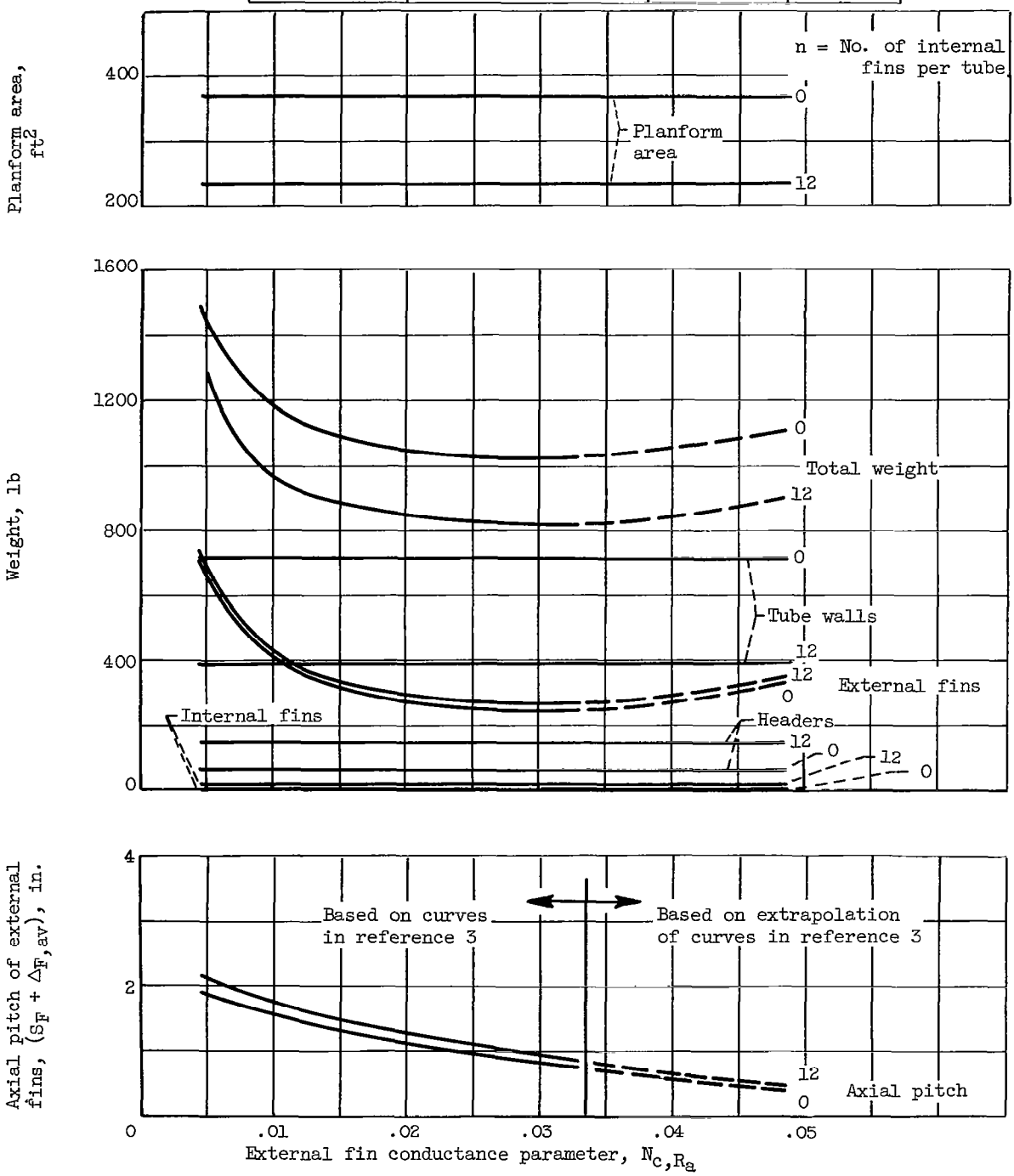

Figure 21. - Effect of N_{c,R_a} and of number of internal fins per tube; circumferential external fins, $R_o/R_a = 4$. Each header split once (see Fig. 2).

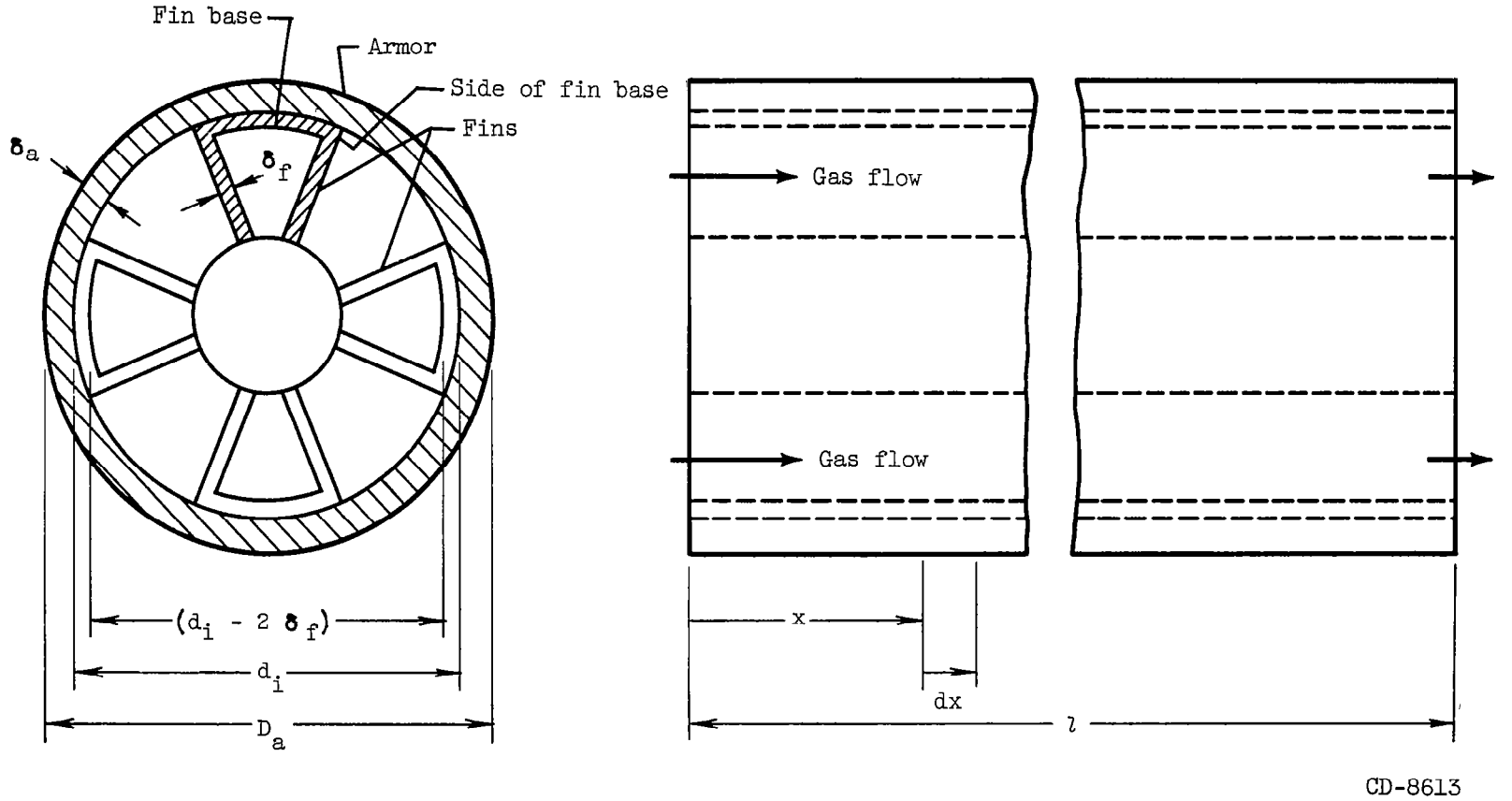

Figure 22. - Internally finned, gas-filled radiator tube.